Monthly Notices
of the
ROYAL ASTRONOMICAL SOCIETY

MNRAS **447,** 2181–2197 (2015) doi:10.1093/mnras/stu2582

On the role of recombination in common-envelope ejections

N. Ivanova,[1⋆] S. Justham[2] and Ph. Podsiadlowski[3]

[1]*University of Alberta, Department of Physics, 11322-89 Ave, Edmonton, AB T6G 2E7, Canada*
[2]*National Astronomical Observatories, Chinese Academy of Sciences, Beijing 100012, China*
[3]*Oxford Astrophysics, Denys Wilkinson Building, Keble Road, Oxford, OX1 3RH, UK*

Accepted 2014 December 3. Received 2014 November 30; in original form 2014 September 5

ABSTRACT

The energy budget in common-envelope events (CEEs) is not well understood, with substantial uncertainty even over to what extent the recombination energy stored in ionized hydrogen and helium might be used to help envelope ejection. We investigate the reaction of a red giant envelope to heating which mimics limiting cases of energy input provided by the orbital decay of a binary during a CEE, specifically during the post-plunge-in phase during which the spiral-in has been argued to occur on a time-scale longer than dynamical. We show that the outcome of such a CEE depends less on the total amount of energy by which the envelope is heated than on *how rapidly* the energy was transferred to the envelope and on *where* the envelope was heated. The envelope always becomes dynamically unstable *before* receiving net heat energy equal to the envelope's initial binding energy. We find two types of outcome, both of which likely lead to at least partial envelope ejection: 'runaway' solutions in which the expansion of the radius becomes undeniably dynamical, and superficially 'self-regulated' solutions, in which the expansion of the stellar radius stops but a significant fraction of the envelope becomes formally dynamically unstable. Almost the entire reservoir of initial helium recombination energy is used for envelope expansion. Hydrogen recombination is less energetically useful, but is nonetheless important for the development of the dynamical instabilities. However, this result requires the companion to have already plunged deep into the envelope; therefore this release of recombination energy does not help to explain wide post-common-envelope orbits.

Key words: binaries: close – stars: evolution – stars: mass-loss.

1 INTRODUCTION

A common-envelope event (CEE) is a brief episode in the life of a binary star during which two stars share an envelope that surrounds their orbit (Paczynski 1976). For the cases in which the envelope is successfully ejected, a CEE might be regarded as a temporary merger, capable of transforming an initially wide binary system into a compact binary. This mechanism is thought to be involved in the production of X-ray binaries, Type Ia supernova progenitors and stellar mass gravitational-wave sources, and is also important in binary models for the progenitors of gamma-ray bursts. However, whilst CEEs are vitally important for a significant fraction of all binaries including the production of a wide variety of energetic stellar exotica, the overall process is still poorly understood.

The overwhelming reasons for our difficulty in understanding CEEs are the complexity of the physical processes involved in each CEE and the extreme ranges in both time-scales (up to a factor of 10^{10}) and length-scales (up to 10^{8}) on which those physical processes take place (Ivanova et al. 2013a). For example, it has been shown first in one-dimensional studies that employed stellar evolution codes (Meyer & Meyer-Hofmeister 1979; Podsiadlowski 2001), and then later reconfirmed by three-dimensional studies that used different hydrodynamical codes (Ricker & Taam 2008; Passy et al. 2012), that for most considered binary configurations the orbital shrinkage, also known as spiral-in, slows down from evolving on a dynamical time-scale – this phase is referred to as the plunge-in – to a thermal time-scale, which is referred to as a 'self-regulated' spiral-in. At this slow stage, modern hydrodynamical codes are no longer capable of treating the physics involved (e.g. convective energy transport), nor are they able to integrate for the expected duration of the stage whilst keeping the most important quantities, such as angular momentum and energy, conserved (Ivanova et al. 2013a).

During the self-regulated spiral-in, the presence of the secondary within the primary star results in energy being deposited into the envelope of the primary. This heating luminosity is normally expected to be dominated by dissipation of orbital energy, i.e. release of gravitational potential energy during the in-spiral, although it is unclear which dissipation mechanism dominates; candidates include viscous friction in differentially rotating layers, tidal friction, and spiral shocks. Another potential source of heating luminosity is accretion on to the secondary star. Convection is expected to advect

⋆ E-mail: nata.ivanova@ualberta.ca

the energy to the surface, and the envelope is expected to adapt its structure to the new total luminosity.

However, the self-regulated spiral-in cannot continue forever, and one of the possible endings is an eventual ejection of the envelope (e.g. via delayed dynamical ejection; Han et al. 2002; Ivanova 2002). Whilst delayed dynamical envelope ejection was reported to take place in those simulations, there were no clear physical reasons for the ejection.

The situation of envelope ejection during a CEE may well be very analogous to the case of asymptotic giant branch (AGB) stars, during which stars eject their own luminous envelopes to form planetary nebulae. The specific instability which causes AGB envelope ejection is still debated, but numerous previous studies exist (see e.g. Paczyński & Zió łkowski 1968; Kutter & Sparks 1972; Sparks & Kutter 1972; Kutter & Sparks 1974; Tuchman, Sack & Barkat 1978, 1979; Fox & Wood 1982; Han, Podsiadlowski & Eggleton 1994; Wagenhuber & Weiss 1994; Soker 2008).

One further similarity between CEEs and AGB stars is that it has been suggested that energy released from the recombination of ionized plasma may help to eject the envelope in both cases (see especially Paczyński & Ziółkowski 1968; Han et al. 1994, 2002; Wagenhuber & Weiss 1994; Han, Podsiadlowski & Eggleton 1995; Ivanova et al. 2013a). Whilst evidence was recently presented which suggests that hydrogen recombination is unlikely to be helpful in unbinding the envelope for a large fraction of CEE events (since recombination happens very near to the photosphere of the already ejected envelope; Ivanova et al. 2013b), our physical understanding of envelope ejection remains highly incomplete. In addition, since helium recombination is expected to occur at higher optical depths than hydrogen recombination, it is particularly plausible that helium recombination could affect the outcome of a CEE (see the discussion in section 3.3.2 of Ivanova et al. 2013a).

This paper systematically examines the physics of envelope ejection and the development of instabilities during CEEs. We adopt a simplified model in order to try to understand the energy budget and the criteria for envelope ejection. The main difference between these calculations and previous work on AGB envelopes is the addition of an artificial heating term. This term is intended to approximately mimic the energy release during the spiral-in of the companion star during CEE in a deliberately simplified way.

We introduce the main quantities that we use for the analysis of instabilities and of the ejection criterion in Section 2 and describe the numerical method for the stellar heating in Section 3. We describe the outcomes for the two limiting cases we use to heat the model star in Sections 4 and 5. In Section 6, we analyse the physical processes that affect the results, including the development of instabilities in the envelope and potential envelope ejection.

2 QUANTITIES

We first introduce several important integrated properties of matter in the envelope: the potential energy $E_{\rm pot}$, the internal energy $E_{\rm int}$, enthalpy $H = E_{\rm int} + P/V$, recombination energy $E_{\rm rec}$ (which we define as the energy which is stored in ionized matter) and kinetic energy $E_{\rm kin}$. In all cases, these are functions of the mass from which the quantity was integrated to the surface:

$$E_{\rm pot}(m_{\rm bot}) = \int_{m_{\rm bot}}^{M} \frac{Gm}{r}\,{\rm d}m; \tag{1}$$

$$E_{\rm int}(m_{\rm bot}) = \int_{m_{\rm bot}}^{M} u\,{\rm d}m; \tag{2}$$

$$H(m_{\rm bot}) = E_{\rm int}(m_{\rm bot}) + \int_{m_{\rm bot}}^{M_*} P/\rho\,{\rm d}m; \tag{3}$$

$$E_{\rm rec}(m_{\rm bot}) = \int_{m_{\rm bot}}^{M} \varepsilon_{\rm rec}\,{\rm d}m; \tag{4}$$

$$E_{\rm kin}(m_{\rm bot}) = \int_{m_{\rm bot}}^{M} \frac{1}{2}v^2\,{\rm d}m. \tag{5}$$

Here M is the total mass of the star, m is the local mass coordinate, r is the radial coordinate, u is the specific internal energy (no recombination energy is taken into account), $\varepsilon_{\rm rec}$ is the specific recombination energy, P is the pressure and ρ is the density. The recombination energy stored in ionized matter can be further described through its three main components, i.e. the energy stored in ionized hydrogen ($E_{\rm rec}^{\rm H\,I}$), singly ionized helium ($E_{\rm rec}^{\rm He\,II}$) and doubly ionized helium ($E_{\rm rec}^{\rm He\,III}$).

The binding energy of the envelope above $m_{\rm bot}$, as is typically used for estimates of the common-envelope (CE) energy budget, is then

$$E_{\rm bind}(m_{\rm bot}) = E_{\rm pot}(m_{\rm bot}) + E_{\rm int}(m_{\rm bot}). \tag{6}$$

The CE energy formalism presumes that this amount of energy must be supplied to eject the envelope, and equates this requirement with the energy available from orbital decay. However, we stress that it is not clear what energy reservoir is truly available (Webbink 2008; Ivanova et al. 2013a) nor how much energy is truly required to expel the envelope and whether that energy is as simply linked to the envelope binding energy as assumed above (Ivanova & Chaichenets 2011).

An exact determination of the post-CE core is very important for the energy balance, as the binding energy of the layers closest to the core can dramatically change the overall envelope binding energy (see e.g. Tauris & Dewi 2001; Deloye & Taam 2010; Ivanova 2011; Ivanova et al. 2013a). Unfortunately, it is not clear whether the outer boundary of a post-CE core would be at the inner mass coordinate of the ejected envelope, $m_{\rm bot}$, as might reasonably be expected (see, e.g. the discussion about a possible post-CE thermal time-scale mass transfer in Ivanova 2011).

Dynamical stability is often characterized using the first adiabatic index Γ_1 (Ledoux 1945):

$$\Gamma_1 = \left(\frac{\partial \ln P}{\partial \ln \rho}\right)_{\rm ad}. \tag{7}$$

The dynamical stability criterion then depends on the pressure-weighted volume-averaged value of Γ_1 (Ledoux 1945; see also Stothers 1999):

$$\langle\Gamma_1(m_{\rm bot})\rangle = \frac{\int_{m_{\rm bot}}^{M_*}\Gamma_1 P{\rm d}V}{\int_{m_{\rm bot}}^{M_*} P{\rm d}V}, \tag{8}$$

such that, if $\langle\Gamma_1(0)\rangle < 4/3$, the whole star is dynamically unstable. Lobel (2001) argued that the envelope in cool giants becomes unstable if $\langle\Gamma_1(m_{\rm env})\rangle < 4/3$, where $m_{\rm env}$ is the bottom of the envelope.

However, it is not clear where $m_{\rm env}$ is located, especially since during a CEE the bottom of the outer convective zone moves upwards in mass coordinate (Ivanova 2002). To help characterize the instability of the envelope, we therefore also introduce three derived quantities:

(i) $m_{\rm uns}$ – the mass coordinate above which the envelope is unstable to ejection, such that $\langle\Gamma_1(m_{\rm uns})\rangle < 4/3$.

(ii) $\Delta m_{\rm env,\,4/3}$ – the mass of the envelope where in each mass shell the local $\Gamma_1(m) < 4/3$.

(iii) $\Delta m_{\rm esc}$ – the mass of the upper part of the envelope in which the expansion velocities exceed the local escape velocity. Of course, the validity of hydrostatic stellar models *after* $\Delta m_{\rm esc}$ starts to increase is questionable.

In this study, we follow the evolution of the above quantities as we inject thermal energy into the envelope of a stellar model. Instead of using time as the main independent variable we will often use the amount of heat which has been added to the star by following both the total heat energy added through the artificial heating, $E_{\rm heat}^{\rm gross}$, and also the total net heat energy that the star received, $E_{\rm heat}^{\rm net}$ – this is the total heat energy added plus all of the nuclear energy that was generated in the star during its heating, $E_{\rm nuc}$, less all the energy that was radiated away from the surface of the star. Another quantity that we trace is the change of the total energy of the core, $\Delta E_{\rm core}$, in the part of the star that is *below* $m_{\rm bot}$.

In a realistic CEE, the distribution of the heat input within the envelope would not be a simple function of radius or mass, and the details would probably depend on many initial conditions such as the mass ratio of the two stars, the initial density profile in the envelope, the degree of corotation at the onset of the in-spiral, how angular momentum is transported through the CE and where this leads to direct kinetic energy deposition, and more (see e.g. Meyer & Meyer-Hofmeister 1979; Podsiadlowski 2001; Ricker & Taam 2012; Ivanova et al. 2013a). One might therefore explore a large parameter space in trying to evaluate the importance of the heat distribution. In this work, we concentrate on two limiting cases: (a) uniform specific heat input throughout the envelope and (b) intense heating in a narrow mass range at the bottom of the envelope.

Note that the outcomes of CEEs are typically estimated by using a standard energy formalism which compares the available energy (in this case the change in the orbital energy $\Delta E_{\rm orb}$) to the binding energy of the envelope. The energy input is presumed to be utilized at some efficiency called $\alpha_{\rm CE} \leq 1$, although it has been common for binary population synthesis codes to resort to 'efficiencies' of greater than unity (typically in lieu of an assumed additional energy source). The broad physical picture underlying this formalism implicitly assumes that the orbital energy is converted into kinetic energy of the envelope. Whilst this is natural during a dynamical time-scale plunge-in, conversion of orbital energy into kinetic energy during a self-regulated spiral-in is definitely indirect.

If the internal energy of the envelope is included in the binding energy calculation, then the standard energy formalism also assumes that the internal energy of the envelope is converted into kinetic energy of the outflow. Whether or not internal energy can be converted into kinetic energy in this way is not established, even less whether the internal energy would be converted with the same efficiency as the energy input from orbital decay.

3 INITIAL CONDITIONS AND NUMERICAL CODE

For the main calculations, in this paper we adopt the same initial stellar model (we briefly describe tests on an alternative model in Section 6.8). The model was chosen to be representative of the low-mass giant stars which are commonly subject to CEEs. This model is a red giant of mass $M = 1.6\,{\rm M}_\odot$ and radius $R = 100\,{\rm R}_\odot$, with core mass $M_{\rm core} = 0.422\,{\rm M}_\odot$ (defined as the hydrogen-exhausted region, where $X < 10^{-10}$; the radius of the core is $\sim$0.02 $\rm R_\odot$). The bottom of the convective envelope is at mass coordinate $M_{\rm ce} = 0.426\,{\rm M}_\odot$ (the distance to the centre is $\sim$0.8 $\rm R_\odot$). The model was created by evolving a $M = 1.6\,{\rm M}_\odot$ zero-age main-sequence star with metallicity $Z = 0.02$ and hydrogen fraction $Y = 0.70$.

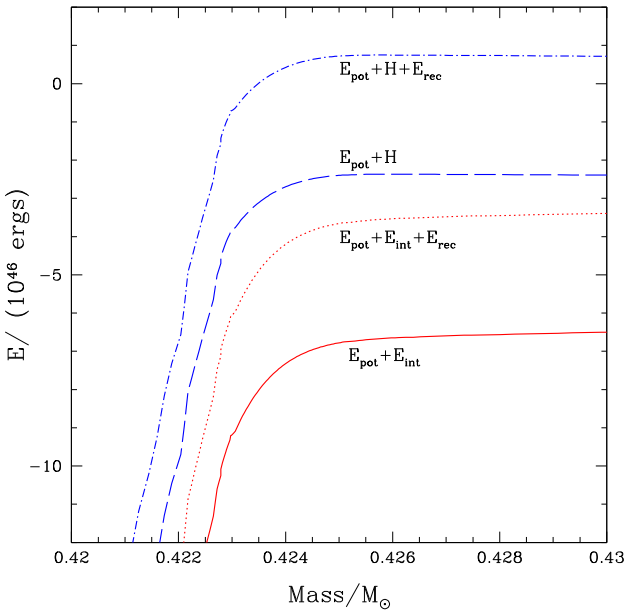

Figure 1. Energies as a function of $m_{\rm bot}$, in the 1.6 $\rm M_\odot$ giant with a radius of 100 $\rm R_\odot$. $E_{\rm pot}$ – the potential energy, $E_{\rm int}$ – the internal energy, H – enthalpy, $E_{\rm rec}$ – the recombination energy reservoir. For definitions see Section 2.

The hydrogen-burning shell in this star, as in all large-radius low-mass giants, is very low in mass and vast in size. Since the radius coordinate changes strongly with the mass coordinate, the potential and thermal energies are strong functions of $m_{\rm bot}$. This can be seen in Fig. 1, in which we show the energies in the region of the star near in mass coordinate to the burning shell and to the bottom of the convective zone. We note that the top curve in Fig. 1 becomes positive near the base of the envelope; this suggests that if enthalpy defines the stability and departure of the envelope, and if the recombination energy reservoir can also be fully utilized, the envelope would have been unbound even before any additional heating. Obviously, this joint condition requires that the recombination energy must become available and hence something would need to trigger recombination.

It is also important to realize that the total binding energy of the star is about 250 times larger than the binding energy of the envelope. Therefore, any thermal feedback between the core and the envelope – including changes in the energy output of the burning shell – may significantly alter the energy balance in the envelope: indeed, only a 1 per cent change in the core binding energy could potentially unbind the envelope! Heating of the envelope during CEEs may well perturb the interior layers sufficiently to cause such a feedback. Hence it seems unlikely that the changes in the energy of a stellar envelope during a CEE could be described properly by assuming that the envelope is a closed system.

The stellar models were evolved using the code and input physics described in Ivanova & Taam (2004). This code is capable of performing both hydrostatic and hydrodynamic stellar evolution calculations. However, for this study, our calculations do not employ the 'dynamical term' in the pressure equation (i.e. hydrostatic equilibrium is assumed). Clearly this will alter our results, especially smoothing over details of pulsational instabilities prior to ejection (see e.g. Wood 1974; Tuchman et al. 1978; Wagenhuber & Weiss

Table 1. Energies in the envelope: uniform heating.

$\Delta E_{\rm heat}^{\rm gross}$	$\Delta E_{\rm heat}^{\rm net}$	$E_{\rm int}+E_{\rm pot}$	$H+E_{\rm pot}$	$E_{\rm rec}$	$E_{\rm rec}^{\rm H\,II}$	$E_{\rm rec}^{\rm He\,II}$	$E_{\rm rec}^{\rm He\,III}$	$E_{\rm kin}$	$\langle\Gamma_1(m_{\rm bot})\rangle$	$\Delta m_{\rm env,\,4/3}$	$m_{\rm unst}$	$\Delta m_{\rm esc}$	$L_*/{\rm L}_\odot$
Unperturbed star													
0.00	0.00	−6.63	−2.35	3.12	2.05	0.08	0.99	0.00	1.62	0.01	1.56	0.00	1594
Case 1: $L_{\rm heat}=10^{45}\,{\rm erg\,yr^{-1}}\equiv 8267\times{\rm L}_\odot$													
1.99	1.85	−4.65	−1.60	3.00	2.04	0.12	0.83	0.00	1.60	0.04	1.51	0.00	2835
10.00	4.35	−1.53	−0.50	2.29	1.90	0.19	0.20	0.00	1.49	0.29	0.97	0.00	9656
Case 2: $L_{\rm heat}=2\times10^{45}\,{\rm erg\,yr^{-1}}\equiv 16535\times{\rm L}_\odot$													
2.00	1.91	−4.59	−1.59	2.99	2.04	0.12	0.83	0.00	1.60	0.04	1.49	0.00	3366
4.00	3.46	−2.73	−0.96	2.64	1.99	0.18	0.47	0.00	1.54	0.15	1.26	0.00	7663
6.00	4.26	−1.41	−0.49	2.09	1.78	0.16	0.15	0.00	1.47	0.35	0.84	0.00	14 617
8.00	4.51	−0.95	−0.32	1.87	1.66	0.13	0.07	0.00	1.43	0.45	0.65	0.00	16 498
10.00	4.55	−0.83	−0.28	1.77	1.60	0.12	0.06	0.00	1.41	0.47	0.60	0.00	17 626
Case 3: $L_{\rm heat}=5\times10^{45}\,{\rm erg\,yr^{-1}}\equiv 41335\times{\rm L}_\odot$													
2.00	1.95	−4.52	−1.58	2.97	2.04	0.13	0.80	0.00	1.59	0.05	1.49	0.00	4229
4.00	3.58	−2.36	−0.85	2.40	1.90	0.20	0.30	0.00	1.55	0.20	1.13	0.00	18 901
5.00	3.91	−1.51	−0.55	1.87	1.59	0.13	0.14	0.01	1.51	0.36	0.71	0.00	38 300
5.50	3.94	−1.26	−0.46	1.66	1.44	0.11	0.11	0.01	1.49	0.40	0.61	0.00	40 643
6.01	3.97	−1.08	−0.39	1.50	1.33	0.09	0.09	0.00	1.48	0.41	0.56	0.00	40 758
6.51	3.99	−0.97	−0.35	1.41	1.26	0.08	0.07	0.00	1.47	0.43	0.53	0.00	40 098
Case 4: $L_{\rm heat}=10^{46}\,{\rm erg\,yr^{-1}}\equiv 82672\times{\rm L}_\odot=1.3\times L_{\rm Edd,\,TS}$													
2.00	1.97	−4.48	−1.57	2.96	2.04	0.14	0.78	0.00	1.59	0.04	1.50	0.00	5028
3.00	2.89	−3.35	−1.20	2.73	2.01	0.19	0.53	0.00	1.57	0.09	1.38	0.00	12 115
4.00	3.61	−2.21	−0.80	2.29	1.85	0.18	0.26	0.05	1.54	0.26	0.96	0.00	44 039
5.00	3.82	−1.37	−0.48	1.64	1.43	0.08	0.13	0.04	1.51	0.35	0.62	0.00	83 600
6.00	3.80	−1.00	−0.35	1.25	1.12	0.05	0.08	0.01	1.48	0.42	0.47	0.00	83 391
8.00	3.83	−0.70	−0.24	0.99	0.91	0.03	0.04	0.00	1.45	0.42	0.45	0.00	81 374
10.01	3.89	−0.55	−0.19	0.90	0.85	0.02	0.03	0.14	1.42	0.42	0.44	0.00	82 271
Case 5: $L_{\rm heat}=10^{47}\,{\rm erg\,yr^{-1}}\equiv 826720\times{\rm L}_\odot=12.8\times L_{\rm Edd,\,TS}$													
2.00	1.99	−4.45	−1.57	2.96	2.05	0.15	0.76	0.10	1.60	0.02	1.52	0.00	7363
2.10	2.10	−4.34	−1.54	2.94	2.05	0.15	0.74	0.12	1.59	0.03	1.51	0.00	8339
2.25	2.24	−4.17	−1.48	2.91	2.05	0.16	0.70	0.19	1.59	0.04	1.50	0.00	10 099
2.50	2.49	−3.88	−1.38	2.86	2.04	0.18	0.64	0.37	1.58	0.05	1.45	0.06	15 372
2.65	2.64	−3.70	−1.32	2.82	2.04	0.18	0.60	0.61	1.58	0.07	1.40	0.09	21 110
2.80	2.78	−3.50	−1.24	2.78	2.04	0.19	0.55	1.00	1.57	0.09	1.35	0.13	31 625

All energies in this table are in units of 10^{46} erg. $L_{\rm heat}$ is the rate of heating which was applied to the star. $E_{\rm heat}^{\rm gross}$ records how much additional energy input was provided to the star, whilst $E_{\rm heat}^{\rm net}$ is the resulting net energy gained by the star (accounting for the nuclear energy input from the core and radiative losses from the surface). $E_{\rm pot}$, $E_{\rm int}$ and H are, respectively, the potential energy, internal thermal energy and integrated enthalpy of the envelope. The reservoir of recombination energy stored in the envelope at each epoch is given by $E_{\rm rec}$, with the contributions from ionized hydrogen, singly ionized Helium and doubly ionized Helium correspondingly given as $E_{\rm rec}^{\rm H\,II}$, $E_{\rm rec}^{\rm He\,II}$ and $E_{\rm rec}^{\rm He\,III}$. $E_{\rm kin}$ is the kinetic energy of the envelope. $m_{\rm bot}$ is the mass coordinate of the base of the envelope. $\langle\Gamma_1(m_{\rm bot})\rangle$ is the pressure-weighted volume-averaged value of Γ_1 in the envelope. $\Delta m_{\rm env,\,4/3}$ is the mass of the envelope where in each mass shell $\Gamma_1(m)<4/3$ (locally). $\Delta m_{\rm esc}$ is the mass of the upper part of the envelope in which the expansion velocities exceed the local escape velocity. $L\star$ is the surface luminosity. For definitions of these quantities see also Section 2.

1994). However, we consider that the effect on the overall energy balance is likely to be far smaller than our current uncertainty. For AGB envelope ejection, Wagenhuber & Weiss (1994) find that including the dynamical terms leads to pulsations and then envelope ejection marginally *earlier* than when assuming hydrostatic equilibrium (in which case ejection occurs without pulsations), i.e. the dynamics of the ejection are substantially different, but the occurrence of an instability is found for both assumptions. For this first study, we feel that consciously avoiding pulsations should clarify the rest of the physics.

4 UNIFORM HEATING OF THE ENVELOPE

To study systematically the envelope response during a self-regulated spiral-in, we first consider simple cases for which the heating is uniformly distributed through the mass of the envelope (at various constant rates). In this set of calculations we also adopt that no mass is lost even if it has a velocity above the escape velocity. We introduced the heating as an additional energy source, constant per gram, in the entire initial convective envelope, with $m_{\rm bot}=M_{\rm ce}=0.426\,{\rm M}_\odot$. The heating is not turned on and off sharply at the edges of this region, but is smoothed such that the specific rate of additional energy input decreases to zero over a transition zone with thickness $0.01\,{\rm M}_\odot$. We calculated sequences for five different rates of heating $L_{\rm heat}$ ranging from 10^{45} to 10^{47} erg yr^{-1} (see Table 1 and Fig. 2).

We estimate that these rates of energy input cover a reasonable range of values for a likely self-regulated spiral-in. This follows if we first assume that this star is in a binary with a companion of $0.3\,{\rm M}_\odot$, and that the self-regulating spiral-in starts when the companion is orbiting somewhat below the region where the original convective envelope was located (though during the spiral-in the envelope expands and so the radiative layer might then be bigger than before the plunge, see Han et al. 2002; Ivanova 2002). In that

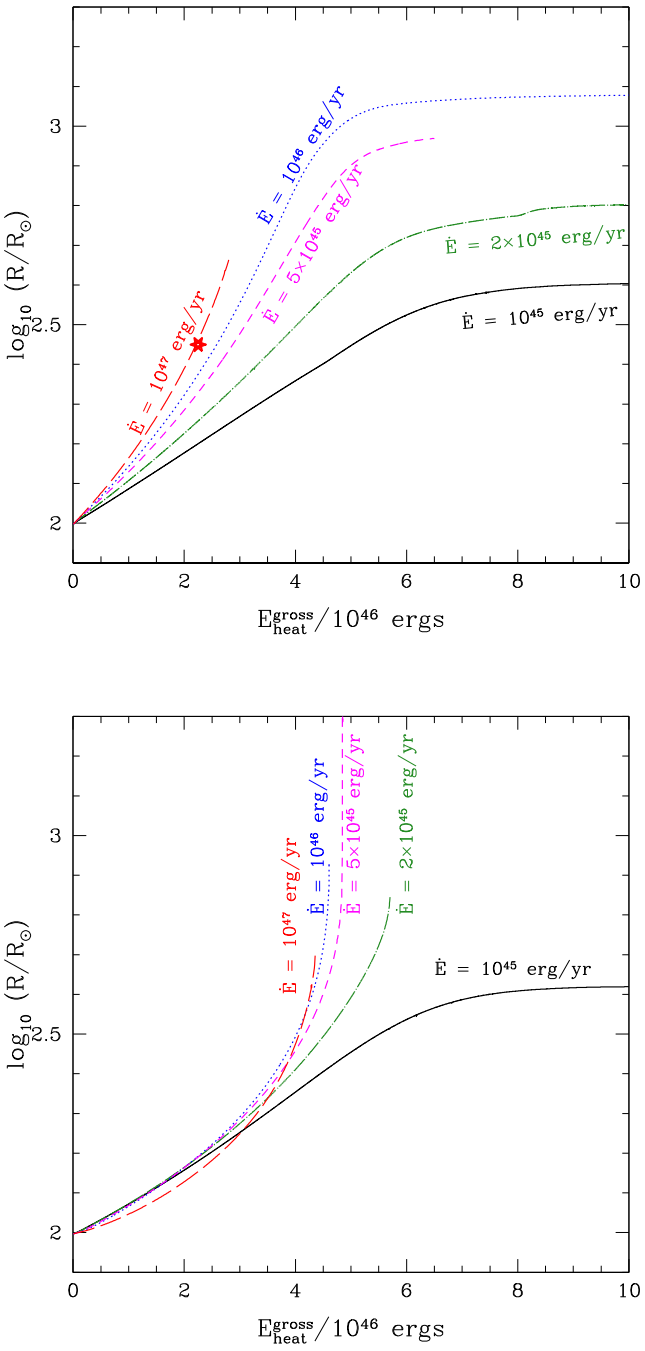

Figure 2. The response of the star – its expansion – as a function of the amount of heat injected into the envelope, for five heating rates. The top panel shows the case when heat is evenly distributed by mass over the whole envelope, and the bottom panel shows that case when the heat is distributed evenly by mass into a shell with mass 0.1 $M_\odot$ at the bottom of the initial convective envelope. For higher heating rates, less integrated energy input is required before ejection occurs, whilst for sufficiently low heating rates the stellar structure can adjust in order to reradiate all of the extra luminosity. In the upper panel, the star symbol marks where equation (12) indicates that the radius expansion is faster than the surface escape velocity.

case, the orbital energy at that stage could be up to of the order of 10^{48} erg. This CEE is destined to eject the envelope leaving a binary behind; however, how compact the final binary is depends on when the envelope is ejected. For a range of time-scales for a self-regulated spiral-in of between 10 and 1000 yr, the heating luminosity can therefore be expected to be between $\approx 10^{45}$ and $\approx 10^{47}$ erg yr^{-1}. Clearly, we would not expect the heating rate to be constant in a real situation, but to depend on the response of the envelope. However, we do anticipate that in a realistic CEE at least the frictional heating could be distributed throughout the differentially rotating envelope, and that the entire envelope could be differentially rotating.

It is convenient to present this additional heat in two different units, both in erg per year (for ease of comparison with the binding energies of the initial star) and in solar luminosities (to compare with the unperturbed stellar luminosity). The Eddington luminosity of our initial model star is $L_{\rm Edd} = 5 \times 10^{37}$ erg s^{-1} $\kappa_{\rm ph}^{-1}$ $(M/{\rm M}_\odot)$, where $\kappa_{\rm ph}$ is the opacity of the photosphere in cm^2 g^{-1}. For comparisons of surface luminosities and the energy input, we adopt Thompson scattering, not the actual material opacity. So we write $L_{\rm Edd,\,TS}$. For our star, $L_{\rm Edd,\,TS} \approx 64300\,{\rm L}_\odot = 7.8 \times 10^{45}$ erg yr^{-1}. Note that, in two of our model sequences, the additional energy input to the star's envelope appears to exceed $L_{\rm Edd,\,TS}$. We also note that the convective turnover time for the envelope of the unperturbed model was calculated as approximately 495 d.

We now discuss the outcomes of our calculations, in order of increasing rate of artificial heating.

4.1 Cases 1 and 2: readjustment and formal stability

Case 1. This model star was heated at a rate of 10^{45} erg yr^{-1}. The stellar structure expanded until the star reached the surface luminosity at which it radiates the same amount of energy as the artificial heating source and the burning hydrogen shell provide together. Most of the initially doubly ionized helium has recombined in the envelope above $m_{\rm bot}$, while only several per cent of the initially ionized hydrogen has done so (see Table 1). Although in Table 1 we show only the model with $\Delta E_{\rm heat}^{\rm gross} = 10 \times 10^{46}$ erg, the star kept evolving in an unchanged state until the total artificial energy input had been at least $\Delta E_{\rm heat}^{\rm gross} = 30 \times 10^{46}$ erg, i.e. about five times the initial binding energy of the star. At that point, we stopped the simulations.

However, except for a tiny mass of about 0.03 $M_\odot$ near to the surface, in which the local $\Gamma_1 > 4/3$, a significant fraction of the envelope is mechanically unstable (see the Table 1 and Fig. 3) and any perturbation may drive its ejection. Since the orbiting binary will very probably cause such a perturbation, it seems reasonable to expect that this part of the envelope could be ejected instead of settling into an eternal self-regulating spiral-in.

Case 2. As in Case 1, the star approaches a stable state in which it radiates away the combined nuclear and heating luminosity. For this higher heating rate, the mass of the envelope that is potentially dynamically unstable is bigger, but so is the mass of the near-surface region with local $\Gamma_1 > 4/3$ (see Fig. 3). This stable near-surface region is more massive because the hydrogen partial ionization zone, H II, has moved inwards. In Fig. 3, we show the location of the partially ionized layers and the way that $\langle\Gamma(m)\rangle$ changes in the envelope. This suggests that any potential dynamical instability is driven by a low Γ_1 in the zone of partial ionization of hydrogen and the first partial ionization zone of helium, He II. Note that in Case 2 *almost the entire envelope* has its helium incompletely ionized, i.e. the helium partial ionization zone is at the bottom of the envelope. This is also traced by the change in $E_{\rm rec}$ – almost all of the recombination energy initially stored in doubly ionized helium, He III, has been released. Another interesting quantity is $\Delta m_{\rm env,\,4/3}$ – this is how much of the envelope mass has its local $\Gamma_1 < 4/3$ – which appears to trace the thickness of the partially ionized hydrogen layer

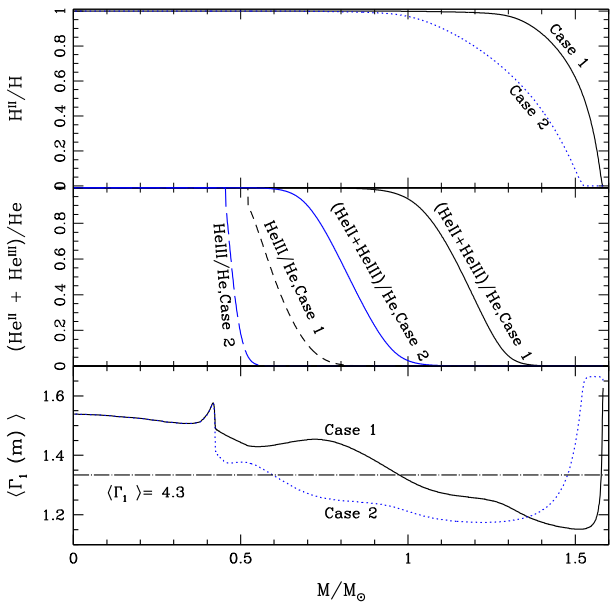

Figure 3. Envelope structure and partial ionization of helium and hydrogen in Cases 1 and 2, uniform heating, at steady-state, in both cases at $\Delta E_{\rm heat}^{\rm gross} = 10 \times 10^{46}$erg. $\langle \Gamma_1(m) \rangle$ is the pressure-weighted volume-averaged value of Γ_1 above the mass coordinate m.

plus the mass where He II >0.01. Almost the entire envelope (all the mass above 0.6 $M_\odot$) is dynamically unstable.

4.2 Case 3: readjustment and then instability

These calculations become unstable after the last model shown in Table 1. In part this instability may well be numerical, and we cannot be sure that it is not entirely numerical. The calculations seem to become undecided over whether the models should converge to either a smaller or a larger radius, each with differently distributed ionization zones. This numerical instability can be suppressed for some time by manual control of the time steps, as the code's automatic time-step choices are not designed for this situation.[1] Nonetheless, we consider that there is a physical reason leading to this instability. The initial dynamical time-scale for the star, before the artificial heating, is $\tau_{\rm dyn} = 0.04$ yr. As the star expands in response to the energy input, $\tau_{\rm dyn}$ also increases. For example, the steady-state expanded stars in Cases 1 and 2 have $\tau_{\rm dyn} \approx 0.5$ yr; in Case 3, at the plateau state, $\tau_{\rm dyn} \approx 1.1$ yr. Each gram of the material in this stellar envelope is heated by $\sim 2 \times 10^{12}$ erg g^{-1} yr^{-1}, while the local specific binding energy of the envelope material at this moment is only $\sim 3 \times 10^{12}$ erg. So in roughly one dynamical time, the outer layers are being heated by more than their binding energy, i.e. the heating of the outermost layers has become dynamical. In addition, most of the envelope mass is already dynamically unstable. We feel this combination indicates that physical envelope ejection is likely, not just a numerical instability. Nonetheless, confirming that this instability is physical will require future calculations in which we follow the dynamics of the envelope.

[1] There appears to be a narrow range of time steps for which the models converge which we are not always able to find. If the time step is too small, the finite numerical precision at which mesh points in each stellar model converge can cause problems, whilst, if the time step is too large, the rate at which recombination energy is released cannot be calculated accurately. (For additional details about the computational complexities in recombination calculations, see Pavlovskii & Ivanova 2014).

4.3 Case 4: a super-Eddington star

The heating rate for this sequence exceeds $L_{\rm Edd,\,TS}$, but this star is able to expand to a luminosity $L > L_{\rm Edd,\,TS}$ (see Fig. 2 and Table 1). This has become possible because the opacities at the surface of this very cold star ($T_{\rm eff} < 3000K$) are *lower* than for Thompson scattering.

In this example, recombination drives the expansion of the star. Table 1 shows that the total release of recombination energy becomes comparable to the rate of heating (e.g. the recombination energy release is 65 per cent of the total heating luminosity – 0.65×10^{46} erg yr^{-1} – between the moments when $E_{\rm heat}^{\rm gross}$ increases from 4 to 5×10^{45} erg). That recombination energy is released in a smaller mass than the heating luminosity and so is locally dominant. We note that this energy mostly comes from hydrogen recombination and is dominant in the mass regions which expand at the fastest rate (see Fig. 4).[2]

This model is on the edge of instability; almost the entire envelope above $m_{\rm bot}$ is unstable, and the star becomes unstable soon after the last model shown in the table. The fact that Case 4 appears to be more stable than Case 3 is in part numerical – due to better fine-tuning of the time steps – and in part because a larger fraction of the outer envelope is radiative: this star has a radiative envelope above 1.44 $M_\odot$, while in Case 3 the outer radiative envelope starts at 1.51 $M_\odot$. So it may be that for uniform heating of the envelope, instability and ejection is not a monotonic function of the rate of energy input – because of the way the heating of the outer regions alters the structure of the outer envelope.

4.4 Case 5: dynamical heating

For our unperturbed star, one needs to add $\sim 3 \times 10^{13}$ erg g^{-1} to the material in the outer envelope to unbind that matter. The uniform heating rate of 10^{47} erg yr^{-1} corresponds to heating of the envelope by 4.3×10^{13} erg g^{-1} yr^{-1}. It is therefore not surprising that this heating will result in the dynamical ejection of the surface layers when the star has expanded such that the dynamical time-scale approaches a year.

We can write the star's expansion with time as a function of heating energy. We use the fact that $L_{\rm heat} \equiv {\rm d}E_{\rm heat}^{\rm gross}/{\rm d}t$ and that, because the heating occurs at a constant rate, $L_{\rm heat} = \Delta E_{\rm heat}^{\rm gross}/\Delta t$. For this case of rapid heating, we also take $\Delta E_{\rm heat}^{\rm net} \approx \Delta E_{\rm heat}^{\rm gross}$ (which

[2] Plots which present 15 different internal quantities for 13 models can be found in the supplementary online material. Five calculations at different heating rates are shown for each of uniform and bottom heating, as well as models X6, X8 and MS015. The plots show luminosity, entropy, the rate of the recombination energy release, the distribution of convective and radiative zones, opacity, the radial coordinate of each mass point, velocity, the ratio of the local luminosity to the local Eddington luminosity in convective regions in which convection would need to be supersonic to carry the predicted convective flux, the 'work' term in the gravitational energy $P/\rho^2 {\rm d}\rho/{\rm d}t$, the time derivative of the internal energy ${\rm d}U/{\rm d}t$, the local value of Γ_1, the pressure-weighted volume-averaged $\langle \Gamma_m \rangle$ integrated inwards from the surface, and the ionization fractions of hydrogen, of singly ionized helium and of doubly ionized helium.

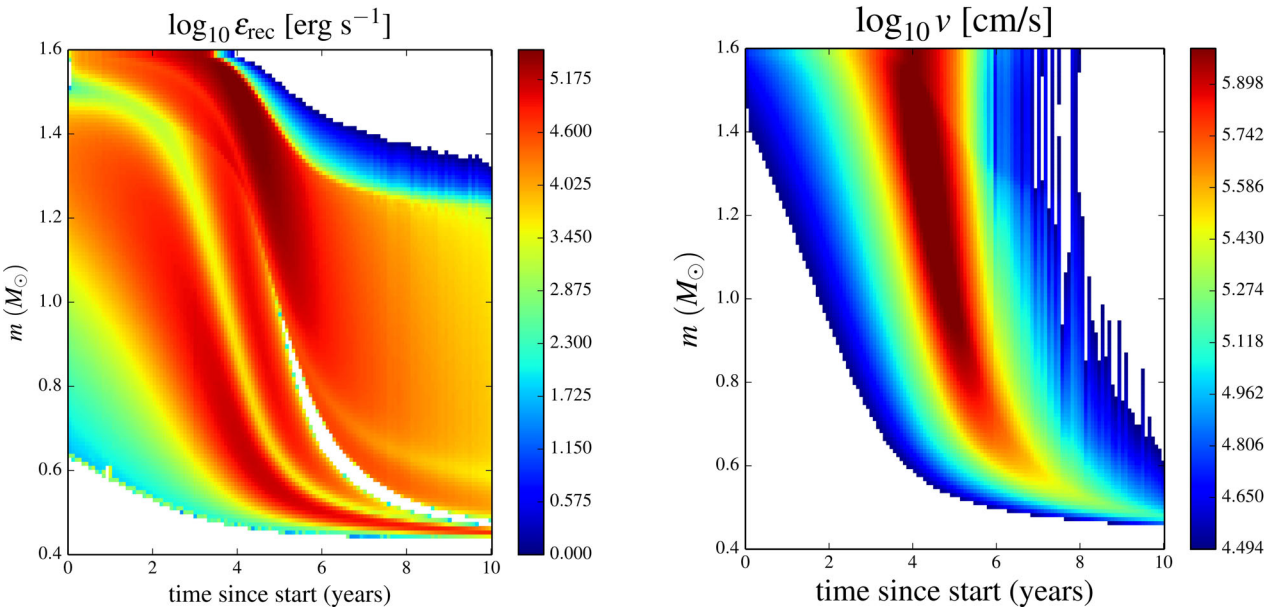

Figure 4. The rate of recombination energy release (the left-hand panel) and expansion velocities (the right-hand panel) in the Case 4 uniform heating.

we have confirmed using the calculations). Then at the moment Δt after the heating had started,

$$\frac{\mathrm{d}R}{\mathrm{d}t} = L_{\rm heat}\frac{\mathrm{d}R}{\mathrm{d}E^{\rm gross}_{\rm heat}} \approx L_{\rm heat}\frac{\Delta R}{\Delta E^{\rm gross}_{\rm heat}}, \quad (9)$$

where ΔR gives the change in radius after time Δt. Since we know that the expansion velocity is increasing with time, the instantaneous expansion velocity must be larger than the mean expansion velocity, i.e. $(\mathrm{d}R/\mathrm{d}t) > (\Delta R/\Delta t)$. In the same units as in Fig. 2, for Case 5, we then have

$$\frac{\mathrm{d}R(\Delta t)}{\mathrm{d}t} > 10 \times \frac{\Delta R/\mathrm{R}_\odot}{\Delta E^{\rm gross}_{\rm heat}/10^{46}\,\mathrm{erg}}\,\mathrm{R}_\odot\,\mathrm{yr}^{-1}. \quad (10)$$

The surface escape velocity for our star is $v_{\rm esc} = 7.8 \times 10^7 \times (R/\mathrm{R}_\odot)^{-1/2}\,\mathrm{cm\,s^{-1}}$. In the unperturbed star $v_{\rm esc} = 78\,\mathrm{km\,s^{-1}}$. As the star expands, the surface escape velocity decreases, and can be written as

$$v_{\rm esc} = \frac{35,300}{\sqrt{R/\mathrm{R}_\odot}}\,\mathrm{R}_\odot\,\mathrm{yr}^{-1}. \quad (11)$$

We can thereby estimate when the star's expansion will be faster than its surface escape velocity

$$\sqrt{\frac{R}{\mathrm{R}_\odot}}\left(\frac{\Delta R}{\mathrm{R}_\odot}\right) > 3530\frac{\mathrm{d}E^{\rm gross}_{\rm heat}}{10^{46}\,\mathrm{erg}}. \quad (12)$$

Note that, because we use $(\mathrm{d}R/\mathrm{d}t) > (\Delta R/\Delta t)$, the speed of expansion will exceed $v_{\rm esc}$ before this point.

From this, we can estimate that free streaming should be expected to start before the star has expanded to ∼900 $\mathrm{R}_\odot$, as the initial binding energy of the envelope is less than 7×10^{46} erg. This estimate is supported by our calculations, as shown in Fig. 2, in which the star symbol marks where the radius derivative satisfies equation (12) above. This moment, at which the star's surface layers start to expand at a speed comparable to the star's current escape velocity, occurs well before the radius reaches 900 $\mathrm{R}_\odot$. At later times, deeper layers reach escape velocity. By the last model shown in Fig. 2, ∼0.13 $\mathrm{M}_\odot$ of the envelope had a velocity higher than the local escape velocity.

We also note that the final envelope is less recombined than in Cases 1 and 2, i.e. more energy is still stored in the ionized plasma when the dynamical instability begins.

4.5 Consequences for CEE from uniform heating

(i) In none of the models was the total *net* heat added to the envelope greater than the initial binding energy of the envelope.

(ii) The additional heat input also leads to a change in the binding energy of the interior. There is no simple but accurate energy balance that considers only the envelope, and the energy balance would strongly depend on the time-scale of the self-regulated spiral-in.

(iii) The outcome depends on the *rate* at which heat was provided, not on the total energy added. Faster heating causes the stellar envelope to begin streaming away at lower $\Delta E^{\rm net}_{\rm heat}$.

(iv) For constant energy deposition rate then, if the heating luminosity is significantly lower than star's Eddington luminosity, the star will adjust to radiate away all of the additional energy input.

(v) The star's envelope can recombine when it attempts to reach a 'steady' state, i.e. readjusting to try to reradiate the additional energy input. Then the helium will have recombined through most of the envelope. Since the second partial ionization zone of helium is rather thick in mass, this seems likely to lead to Cepheid-type pulsations; note that we cannot obtain normal Cepheid pulsations naturally with the hydrostatic code we used.

One large inconsistency with this model is that the heating is uniform all the way to the surface. This causes heating of the outer envelope on a dynamical time-scale, which leads to instabilities. In a more realistic situation, this surface heating would not occur.

5 BOTTOM HEATING

For this set of simulations, the additional energy input was introduced into the bottom 0.1 $\mathrm{M}_\odot$ of the initial convective envelope. This situation more closely resembles the local heating during a phase of self-regulating spiral-in, albeit it lacks subsidiary heating of the surface layers that would be present in a more realistic case of CEEs. We injected the same total amount of energy as in the case

of uniform envelope heating, again uniformly distributed in mass but only spread over the 0.1 $M_\odot$ shell.

Overall, this more concentrated bottom heating is significantly more effective in causing the stellar envelope to stream out at a smaller imposed $\Delta E_{\rm heat}^{\rm gross}$.

The upper and lower extreme heating rates (Case 1 and Case 5) produce outcomes which are qualitatively similar to the corresponding simulations with uniform heating. In Case 1, the star adjusts to enable eternal self-regulation, and in Case 5 the envelope is dynamically ejected. All the intermediate simulations (Cases 2, 3 and 4) also lead to dynamical ejection after $\Delta E_{\rm heat}^{\rm net} \approx 4.5 \times 10^{46}$. At that moment, $\Delta m_{\rm env,\,4/3} \approx 0.5$ for all models. The envelopes have $\Gamma_1 < 4/3$ down to 0.5 $M_\odot$ and $\Gamma_1 = 1.4$ down to $m_{\rm bot}$.

The development of the envelope expansion is smooth and does not cause obvious numerical problems until the local velocities exceed their local escape velocities; at this point, we cannot fully trust the stellar models anymore (although we still list the output in the table). We also note that the rate of the total energy release provided by recombinations at this moment exceeds $L_{\rm Edd,\,TS}$ (see Fig. 7 and also the discussion in Section 6.3). Strictly speaking, the models may become unreliable somewhat earlier than that, when the local expansion velocities exceed the convective velocities.

We can identify the following stages of envelope ejection (see also Fig. 5).

(i) Expansion of the inner envelope leads to cooling. When the cooling is sufficient, this causes helium recombination.

(ii) Helium recombination proceeds and can sometimes produce a higher rate of energy input than the heating which led to the recombination: $\dot{E}_{\rm rec} > \dot{E}_{\rm heat}^{\rm gross}$. Heating of the layers where helium has already recombined causes more rapid expansion than before recombination. The envelope above the helium recombination zone expands rather uniformly.

(iii) Hydrogen recombination then moves inwards in mass as the envelope expands. This can also release energy at a higher rate than the heating. Because this occurs in the outer parts of the envelope, they are the most affected by this release of energy, and so the outer layers begin to expand rapidly. Hydrogen recombination and first helium recombination zones are quickly moving inwards in mass. This is the stage during which the envelope acquires a kinetic energy above 10^{44} erg and some mass can start moving with a speed above its local escape velocity.

For all of the models calculated for this paper, almost all of the energy which is initially stored in ionized helium was used to help expand the envelope. We are therefore tempted to conclude that it is normally true that the vast majority of helium recombination energy is useful in envelope expansion. However, a smaller fraction of the energy stored in ionized hydrogen is used to expand the envelope – we estimate between a few per cent and 60 per cent – and we stress that hydrogen recombination is *less* efficient in the case of runaway envelopes than in cases of self-regulated expansion (see also the discussion on the role of recombination in Section 6.3).

We find that in all models which ended with a runaway, the rate of energy input from the recombination of helium at each epoch exceeds that from hydrogen recombination. When the recombination zone approaches the bottom-heated layer then the relative rate of recombination energy release between models follows the relative differences in the heating rate between those models. For the self-regulated models, the maximum rate of recombination energy release from helium also changes with the heating rate, albeit for those models the rate of energy release from hydrogen recombination can be higher than that from helium at the same instant. This

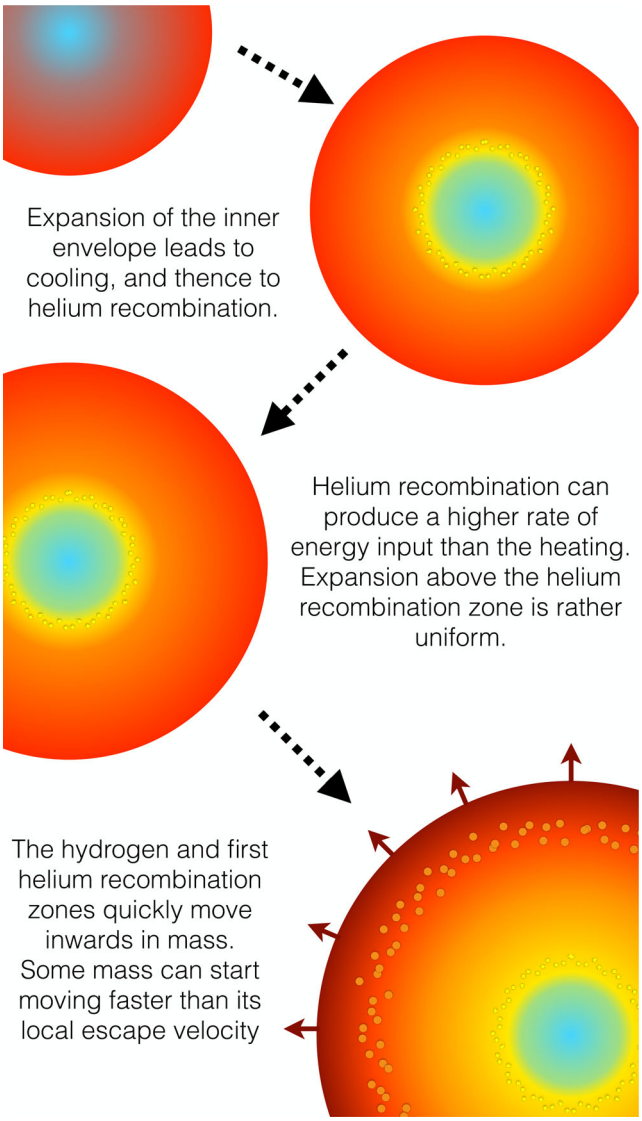

Figure 5. The stages of envelope ejection in the bottom-heating case.

leads us to the conclusion that one of the most important effects of the heating is to trigger helium recombination and that the local rate of that helium recombination depends strongly on the heating rate.

5.1 Testing for the moment of instability

Since the instability takes a finite time to develop, we tested whether our heating had been applied for longer than necessary to trigger the instability. Perhaps the constant heating in our earlier simulations had continued even after the envelope had become unstable?

One could expect a star to develop dynamically instability on its dynamical time, which is about a year for our expanded stars. For Case 4, a year of heating implies a different gross energy input by $\approx 10^{46}$ erg!

For this test, we took several stars from the heating sequence and let them evolve freely, without further heating, and studied whether the star continued to expand and eject the envelope or remained bound and contracted back towards the initial configuration. In the Case 4 bottom-heating sequence, the star with $\Delta E_{\rm gross}^{\rm heat} = 4.62$ (see Table 2) is the last star that contracts when heating is switched off. Later models in the sequence keep expanding. This demonstrates

Table 2. Energies in the envelope: bottom heating.

$\Delta E_{\rm heat}^{\rm gross}$	$\Delta E_{\rm heat}^{\rm net}$	$E_{\rm int}+E_{\rm pot}$	$H+E_{\rm pot}$	$E_{\rm rec}$	$E_{\rm rec}^{\rm H\,II}$	$E_{\rm rec}^{\rm He\,II}$	$E_{\rm rec}^{\rm He\,III}$	$E_{\rm kin}$	$\langle\Gamma_1(m_{\rm bot})\rangle$	$\Delta m_{\rm env,\,4/3}$	$m_{\rm unst}$	$\Delta m_{\rm esc}$	$L_*/{\rm L}_\odot$
Unperturbed star													
0.00	0.00	−6.63	−2.35	3.12	2.05	0.08	0.99	0.00	1.62	0.01	1.56	0.00	1594
Case 1: $L_{\rm heat}=10^{45}\,{\rm erg\,yr^{-1}}\equiv 8267\times{\rm L}_\odot$													
2.00	1.87	−4.63	−1.60	2.98	2.04	0.12	0.81	0.00	1.60	0.04	1.51	0.00	2625
4.00	3.36	−2.93	−1.01	2.73	2.02	0.18	0.53	0.00	1.55	0.11	1.36	0.00	4691
10.00	4.40	−1.39	−0.47	2.20	1.86	0.18	0.17	0.00	1.47	0.33	0.92	0.00	9625
Case 2: $L_{\rm heat}=2\times10^{45}\,{\rm erg\,yr^{-1}}\equiv 16535\times{\rm L}_\odot$													
2.00	1.95	−4.54	−1.57	2.98	2.04	0.13	0.80	0.00	1.60	0.04	1.50	0.00	2673
4.00	3.66	−2.53	−0.88	2.63	2.00	0.19	0.44	0.00	1.54	0.15	1.29	0.00	5540
5.00	4.31	−1.55	−0.53	2.28	1.90	0.19	0.20	0.00	1.49	0.31	1.00	0.00	9383
5.50	4.51	−1.05	−0.36	1.97	1.73	0.14	0.10	0.00	1.44	0.44	0.71	0.00	13 929
5.70	4.53	−0.77	−0.26	1.70	1.55	0.09	0.05	0.04	1.39	0.50	0.52	0.00	22 661
Case 3: $L_{\rm heat}=5\times10^{45}\,{\rm erg\,yr^{-1}}\equiv 41335\times{\rm L}_\odot$													
2.00	1.98	−4.52	−1.58	2.96	2.04	0.13	0.79	0.00	1.59	0.04	1.50	0.00	2655
3.99	3.85	−2.29	−0.80	2.56	1.99	0.20	0.37	0.00	1.53	0.18	1.23	0.00	6328
4.51	4.29	−1.59	−0.55	2.29	1.91	0.18	0.20	0.01	1.49	0.31	1.00	0.00	10 496
4.61	4.37	−1.44	−0.50	2.21	1.87	0.17	0.16	0.01	1.48	0.34	0.89	0.00	12 324
4.71	4.44	−1.27	−0.44	2.11	1.82	0.16	0.13	0.02	1.46	0.41	0.80	0.00	15 208
4.81	4.50	−1.06	−0.37	1.96	1.74	0.13	0.09	0.10	1.44	0.47	0.68	0.00	21 987
4.86	4.52	−0.91	−0.31	1.81	1.65	0.10	0.07	0.71	1.41	0.50	0.54	0.29	33 605
Case 4: $L_{\rm heat}=10^{46}\,{\rm erg\,yr^{-1}}\equiv 82672\times{\rm L}_\odot=1.3\times L_{\rm Edd,\,TS}$													
2.01	2.00	−4.48	−1.57	2.96	2.04	0.13	0.78	0.00	1.59	0.04	1.50	0.00	2637
4.01	3.94	−2.11	−0.75	2.49	1.98	0.20	0.31	0.01	1.52	0.20	1.16	0.00	7268
4.50	4.38	−1.33	−0.47	2.14	1.85	0.16	0.14	0.10	1.47	0.41	0.80	0.00	17 473
4.60	4.45	−1.10	−0.39	1.98	1.76	0.12	0.09	0.50	1.44	0.49	0.66	0.14	28 370
4.62	4.46	−1.04	−0.37	1.93	1.73	0.11	0.08	1.32	1.43	0.49	0.61	0.37	33 629
4.64	4.47	−0.96	−0.34	1.85	1.69	0.10	0.07	3.21	1.41	0.51	0.54	0.63	42 871

All energies in this table are in units of 10^{46} erg. For descriptions of the variables see Table 1 and Section 2.

that, in this case, the moment when the star has become unstable and our final model are not very different.

5.2 Testing for the role of the recombination energy input

To investigate the role of the recombination energy release in the outcome of heating, we tested what happens in an imaginary situation in which recombination energy cannot be used. We recalculated Cases 2, 3 and 4 with bottom heating, but instantaneously removed the recombination energy from the gravitational energy source in the stellar structure equations. However, we anticipate that removal of the recombination energy could introduce numerical instabilities; therefore, these calculations should be considered less trustworthy than our main results.

All of these modified calculations produced results which were different from the unmodified case. For the bottom-heated Case 4 with no recombination energy input – where helium recombination would have played a smaller role in the total energy budget than in Case 2 – we found slower radius expansion for equivalent $\Delta E_{\rm heat}$ than for the Case 4 calculations which included recombination energy input (for either uniformly distributed or bottom-concentrated heating). However, the expansion of this star is still very fast compared to that of the star in Case 2. In the final converged time step, this stellar model possesses a radius smaller than in either of the standard Case 4 models. Hence, although the envelope is strongly formally dynamically unstable at this point, it is not clear to us whether the star would experience dynamical instability during a self-regulated spiral-in or eject the envelope during runaway expansion.

The difference between Case 3 models with and without recombination energy release was similar to the situation in Case 4. That is, the stellar expansion was slower than in both the bottom and uniformly heated Case 3, however, envelope expansion still runs away after the hydrogen recombination front begins to propagate inwards.

The biggest difference between the cases with and without recombination energy was in Case 2, in which recombination energy would have played a stronger role compared to the other cases. When the recombination energy was removed, the star did not run away and entered a self-regulated spiral-in, reaching the same radius as in the Case 2 uniform heating. However, the envelope is slightly more formally unstable than in the standard Case 2, having $\langle\Gamma_1(m_{\rm bot})\rangle = 1.39$ at $\Delta E_{\rm heat}^{\rm gross} = 8.4\times10^{46}$ erg (which is the last converged model).

We conclude that this definitively demonstrates that helium recombination energy affects the change of the stellar structure during a CE spiral-in and thereby alters the outcome of the CE phase.

5.3 Testing for the role of the location of the heating source

We tested what would happen if heating was applied at the same specific rate (i.e. the same $\varepsilon_{\rm heat}$ in erg g^{-1}), but when the location of the heating was changed. For this test, we chose to shift the bottom boundary outwards by −0.02, 0.05, 0.1 and 0.15 M$_\odot$ compared to our standard bottom heating. We also chose the Case 2 rate of heating because this is the case for which changing between uniformly distributed and bottom heating qualitatively alters the outcome from self-regulated to runaway expansion. The first three

changes of location made little difference to the results, but when the inner boundary was moved outwards by $0.15\,M_\odot$, then the stellar expansion started earlier, increasing the star's surface luminosity. In this calculation, the model approached the self-regulated solution (we will refer to this model as the MS015 version of Case 2 bottom heating).

5.4 Testing different heating concentrations

We also tested the change in outcome when the same total rate of heating was concentrated within a different amount of mass. Again we chose to compare to the Case 2 bottom-heating model, in which the heat was injected into a $0.1\,M_\odot$ layer. In models with uniform heating, the energy input is distributed over almost $1.4\ M_\odot$ of envelope. For this test, we calculated examples where the Case 2 rate of energy input was distributed in layers with masses of 0.025, 0.05, 0.2, 0.4, 0.6 and $0.8\,M_\odot$, with inner edges located at the bottom of the convective envelope. In each of the first four of those examples (i.e. with the specific heating rate up to four times higher or four times lower than the baseline model), the radius evolution did not differ at all from the standard Case 2 bottom-heating calculation.

When the mass of the heated layer was increased to $0.6\,M_\odot$ (we will refer to this model as the X6 version of Case 2 bottom heating), then the radius evolution was slightly different – with earlier expansion as the effects of heating reached the surface earlier. This calculation also appears to almost reach a self-regulated state, but fails to do so (see more in Section 6.6). The last converged model has a radius which is almost the same as in the comparison calculations with a smaller heated mass (including the standard Case 2 bottom-heating calculation), but which is larger than the steady self-regulating radius reached by the uniformly heated calculation with the Case 2 energy input rate.

When the energy input was distributed in $0.8\,M_\odot$ (which we shall call the X8 version of Case 2 bottom heating), the initial expansion of the star was just slightly slower than for the uniformly heated Case 2 and slightly faster than for the standard bottom-heated Case 2 calculations. At $\Delta E_{\rm heat}^{\rm gross} \approx 5 \times 10^{46}$ erg, the stellar expansion overtook the uniform case and the model reached a nearly self-regulated radius at $\Delta E_{\rm heat}^{\rm gross} \approx 5.5 \times 10^{46}$ erg, slightly earlier than in the uniformly heated calculation. However, the self-regulation was not perfect, and the star continued to expand very slowly. This expansion eventually ran away at the same radius at which the runaway happened for the calculations with smaller $\delta m_{\rm heat}$.

6 DISCUSSION OF PHYSICAL PROCESSES

6.1 Convective and radiative regions and an entropy bubble

There is a striking difference between uniform and bottom heating in the internal energy transport: the distribution of radiative and convective zones. For uniform heating, convection halts. This is due to a snowball effect which is triggered by heating throughout the envelope. That heating leads to a temperature increase and, accordingly, to a small decrease in opacities, decreasing the radiative gradient. As radiation plays an increasing role in transporting the energy and convection becomes relatively less efficient (see examples in Fig. 6), an internal radiative zone is created. As a result, the local specific entropy increases, creating an 'entropy bubble'. The growth of this entropy, and specifically the presence of a negative entropy gradient (i.e. $\mathrm{d}s/\mathrm{d}m < 0$) leads to the re-establishment of convection. Even though the convection zone again extends further inside, it never penetrates as deep as it had done before. At the surface, once hydrogen recombination starts, each of our uniform-heating models develops a radiative zone.

By contrast, the convective zone for bottom-heated models does not change with time, except for the creation of a small surface radiative zone in some cases. We note that this implies that the structure of the envelope during the evolution of the bottom-heated models remains close to isentropic, but that this is not generally true for uniform heating. We have checked that the absolute value of the adiabat in bottom-heated models is almost constant in time. Hence the envelope expansion caused by bottom-concentrated heating is close to adiabatic, whilst uniform heating leads to a strongly non-adiabatic envelope expansion. The exception is Case 5 of uniform heating, for which the specific entropy is also mostly uniform throughout the envelope, most likely because the duration of the evolution is too short for it to change. In Section 6.3, we argue that this difference in 'adiabatic' versus 'non-adiabatic' envelope expansion is significant in understanding the differing usefulness of recombination energies.

6.2 The location of the photosphere

Once the hydrogen recombination front begins to move inwards from the surface, the opacities of the outer layers drop dramatically. It is these layers with recombined hydrogen that become radiative. Sometimes as much as the outer $0.2\,M_\odot$ can contain neutral hydrogen and be radiative. Moreover, a significant fraction of that mass can be optically very thin and is likely located above the photosphere of the star.

This is qualitatively similar to the expected structure of a red supergiant, with a cool extended atmosphere and convection starting to play a role in the energy transport only at large optical depths (see Paczyński 1969). It is not intuitively clear whether any simple photospheric condition can be used to model such stars. In the past, it was even argued that a zero boundary condition at $\tau = 0$ with $L = 8\pi\sigma R^2 T_0^4$ should be used (Paczyński 1969, see this paper for how to obtain the radiative temperature gradient in the atmosphere with this boundary condition). Here T_0 is the temperature at $\tau = 0$. However, it has also been shown that, for these optically thin atmospheres, the chosen boundary condition does not affect the solution as long as the atmospheric opacities are sufficiently low (Paczyński 1969). Although the stellar structures we obtain are no more inconsistent than standard stellar models of red supergiants, we realize that it may be interesting for future studies to investigate how modified atmospheric models affect our results.

The work of Ivanova et al. (2013b) suggested that the recombination of hydrogen in a large fraction of the envelope mass did not occur until *after* the envelope was ejected. This may well still be consistent with our results here if the remainder of the envelope is rapidly ejected. We note that, as discussed in Section 1, our neglect of the dynamical terms seems likely to lead to systematically *later* ejection in these calculations than in reality. So perhaps in reality the hydrogen recombination front has less time to propagate inwards before envelope ejection.

6.3 Recombination energies

We introduce the recombination luminosities

$$L_{\rm rec,H} = \int_M \varepsilon_{\rm rec,H} \mathrm{d}m \qquad (13)$$

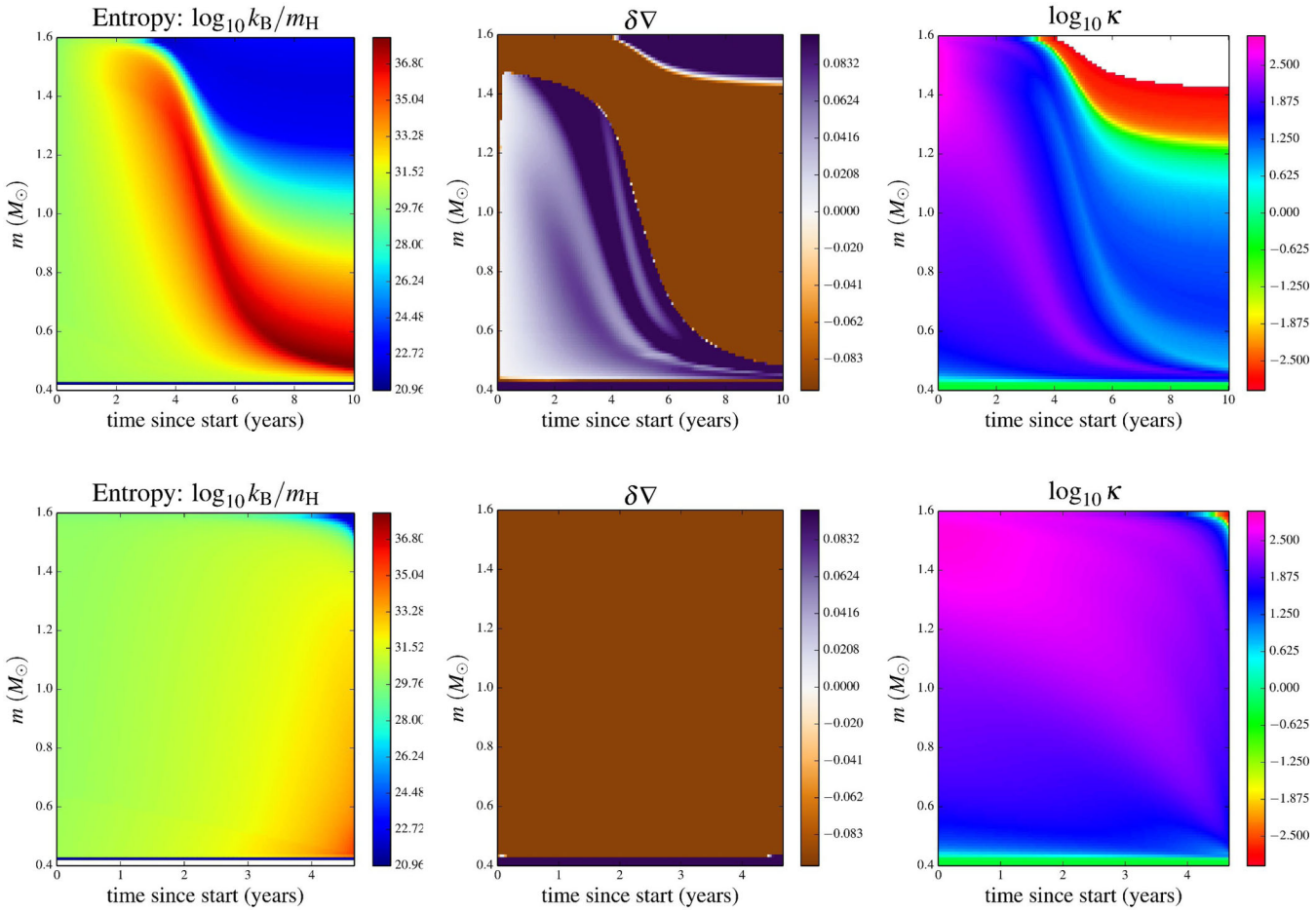

Figure 6. The entropy (the left-hand panels), radiative and convective zones (the middle panels) and opacities (the right-hand panels) for the Case 4 heating rate when adopting both uniform heating (the top panels) and bottom heating (the bottom panels). The radiative and convective zones are shown as the difference in gradients $\delta\nabla = \nabla_{ad} - \nabla_{rad}$, where brown indicates convective regions and shades of purple show radiative regions. To clarify the presentation of the gradients, we truncated the value of $\delta\nabla$ at -0.1 in convective regions and at 0.1 in radiative regions.

and

$$L_{\rm rec,He} = \int_M \varepsilon_{\rm rec,He} {\rm d}m. \tag{14}$$

Here $\varepsilon_{\rm rec,\,H}$ and $\varepsilon_{\rm rec,\,He}$ are local specific energy generation rates due to the recombination of hydrogen and helium (respectively).

We also define the 'dynamical' luminosity as the ratio of the binding energy of the envelope to the dynamical time-scale of the star, $\tau_{\rm dyn}$:

$$L_{\rm dyn} = \frac{E_{\rm bind}(m_{\rm bot})}{\tau_{\rm dyn}}. \tag{15}$$

For this estimate, we use $\tau_{\rm dyn} = \sqrt{R^3/GM}$.

In Fig. 7, we show the recombination luminosities $L_{\rm rec,\,H}$ and $L_{\rm rec,\,He}$, as well as the ratio of the total recombination luminosity $L_{\rm rec} = L_{\rm rec,\,H} + L_{\rm rec,\,He}$ to the star's dynamical luminosity. We find that in all the models where the envelope expansion runs away, the total recombination luminosity exceeds the dynamical luminosity. This helps to explain why those stars cannot remain in equilibrium. In this 'runaway' regime, the recombination luminosity is predominantly provided by hydrogen recombination, which increases sharply just before the expansion runs away. The rapid growth of $L_{\rm rec,\,H}$ appears to drive a similar increase in $L_{\rm rec,\,He}$. Before the onset of this runaway behaviour, the evolution of $L_{\rm rec,\,He}$ is almost independent of how the heating regions are distributed, only on the total energy input.

The maximum $L_{\rm rec,\,H}$ with which we see the star enter a self-regulated state is $\log L_{\rm rec,\,H}/{\rm L}_\odot = 4.6$ (the Case 4 uniform heating). For any model, in which we have calculated $\log L_{\rm rec,\,H}/{\rm L}_\odot > 4.6$, we find that the envelope expansion starts to run away. The connection between recombination luminosity and the mass of stellar material that is recombining is

$$L_{\rm rec,H}/{\rm L}_\odot \approx 2.1 \times 10^5\ X \dot{M}_{\rm rec,H}[{\rm M}_\odot\ {\rm yr}^{-1}] \tag{16}$$

and

$$L_{\rm rec,He}/{\rm L}_\odot \approx 3.2 \times 10^5\ Y \dot{M}_{\rm rec,He}[{\rm M}_\odot\ {\rm yr}^{-1}], \tag{17}$$

where X and Y are the mass fractions of hydrogen and helium, and $\dot{M}_{\rm rec,H}$ and $\dot{M}_{\rm rec,He}$ are the rates at which hydrogen and helium recombine, in ${\rm M}_\odot\ {\rm yr}^{-1}$. When $\log L_{\rm rec,\,H} = 4.6$, as in the case described above, the recombination of hydrogen proceeds at a rate of $\sim 0.3\,{\rm M}_\odot {\rm yr}^{-1}$. Therefore, the associated recombination front is moving inwards through the envelope on a time-scale almost as short as the dynamical time-scale of the expanded star. We note that for these 'self-regulated' stellar structures, or when the expansion starts to run away, the hydrogen recombination zones are at an optical depth significantly more than 1. Because the recombination front is not thin, there is no single unambiguous

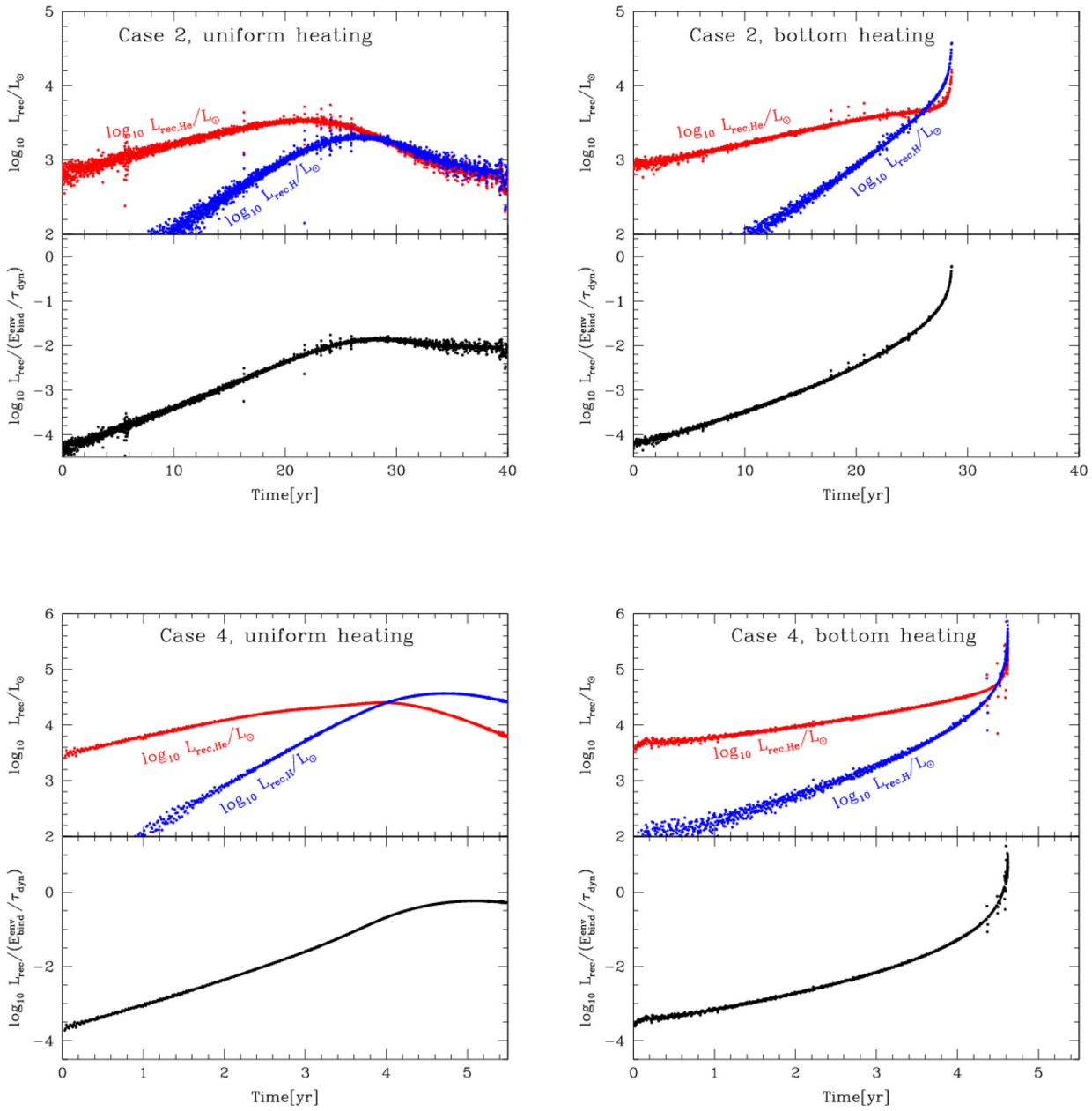

Figure 7. The role of recombination luminosities in Cases 2 (upper pairs of plots) and 4 (bottom pairs of plots), uniform heating (left) and bottom (right) heating. The top panels in each case show the energies provided by hydrogen $L_{\rm rec,\,H}$ (blue) and helium $L_{\rm rec,\,He}$ (red) recombination. The bottom panels show the ratio between the total recombination luminosity $L_{\rm rec} = L_{\rm rec,\,H} + L_{\rm rec,\,He}$ and the 'dynamical' luminosity – which we define as the current binding energy of the envelope divided by the envelope's current dynamical time. Note that all of the recombination luminosities are derived quantities which were not used during the evolutionary calculations. The noise is mainly due to the way in which the changes in the ionization states between models were calculated during the post-processing, with larger noise when the models were remeshed by mass.

way to define the depth of the recombination zones. The simulations show $\varepsilon_{\rm rec} < 10^3\,{\rm erg\,g^{-1}s^{-1}}$ when the ionization fraction is below 0.1, which is at $\tau \lesssim 500$. We also see $\varepsilon_{\rm rec} \lesssim 10^2\,{\rm erg\,g^{-1}s^{-1}}$ at $\tau \lesssim 50$. Hence, is it plausible that a significant fraction of the hydrogen recombination energy is used to expand the star in these situations.

Helium recombination energy is usually almost fully utilized for driving envelope expansion. Only at each extreme of the heating rates we considered, a large fraction of this energy was not released by the end of the simulations. For Case 1, the rate of energy input is so small that $\dot{M}_{\rm rec,He}$ is also very small. For Case 5 with uniform heating, the expansion of the stellar surface runs away before the inner layers expand sufficiently to start recombining (i.e. 'dynamical heating' of the surface).

But why does the expanding star sometimes survive hydrogen recombination whilst for other models the expansion runs away? Consider the Saha equation for pure hydrogen, where we denote the ionization fraction of hydrogen as y =H II/H:

$$\frac{y^2}{1-y} = 4\times10^{-9}\left(\frac{T}{\rm K}\right)^{3/2}\left(\frac{\rm gcm^{-3}}{\rho}\right)\exp\left(-\frac{1.58\cdot10^5\,\rm K}{T}\right) \equiv F(\rho,T). \quad (18)$$

Here, T is the temperature in K and ρ the density in gcm^{-3}. The left-hand side of the equation, $y^2/(1-y)$, monotonically changes with y. When the right-hand side of the equation ($F(\rho, T)$) decreases, the ionization fraction y also decreases. Hydrogen recombination starts with decreasing $F(\rho, T)$, and hydrogen becomes half recombined when $F(\rho, T) = 0.5$. While we anticipate that in a complete equation of state (EOS), $F(\rho, T)$ has a more complicated form due to the presence of helium and free electrons from other elements, the dependence on the temperature and density for hydrogen ionization fractions is broadly determined by the simple Saha equation for pure hydrogen as above, since helium ionization is very small until hydrogen is almost fully ionized, and hence helium does not provide many free electrons. The density and temperature, through $F(\rho, T)$, therefore determine the degree of hydrogen ionization.

For this analysis, we will assume a simple power-law EOS of the form $T \propto \rho^x$. Here, $x = 2/3$ would correspond to adiabatic changes of a monatomic ideal gas, and so the term $T^{3/2}/\rho$ in $F(\rho, T)$ is constant in case of an adiabatic change. If the entropy of the material increases, the change is non-adiabatic, and this situation could be described by using $x < 2/3$. Plasma with a higher entropy has a larger $F(\rho, T)$ and is less recombined.

The rate of recombination energy release from hydrogen is proportional to the change in ionization fraction: $\varepsilon_{\mathrm{rec,\,H}} \propto -\,\mathrm{d}y/\mathrm{d}t$. From equation (18) we obtain

$$\begin{aligned}\frac{\mathrm{d}y}{\mathrm{d}t} &= \frac{(y-1)^2}{(2-y)y}\left(\frac{3}{2}x - 1 + x\frac{1.58\cdot 10^5\,\mathrm{K}}{T}\right)\frac{\mathrm{d}\ln\rho}{\mathrm{d}t}F(\rho,T)\\ &\approx 6.3\times 10^{-4}\frac{(y-1)^2}{(2-y)y}\left(\frac{T}{\mathrm{K}}\right)^{1/2}\left(\frac{\mathrm{gcm}^{-3}}{\rho}\right)\\ &\quad\times\exp\left(-\frac{1.58\times 10^5\,\mathrm{K}}{T}\right)x\frac{\mathrm{d}\ln\rho}{\mathrm{d}t}. \qquad (19)\end{aligned}$$

We can now use the framework described above to examine the differing outcomes of envelope expansion (as parametrized by decreasing density). We have previously argued that the two relevant limiting cases are adiabatic expansion and expansion with entropy increase (see Section 6.1). For the same expansion rate ($\mathrm{d}\ln\rho/\mathrm{d}t$), at every instant, the temperature in the adiabatic case will be higher. The value of x is also higher for adiabatic expansion than for expansion with entropy increase. Therefore, equation (19) helps to explain why the recombination energy release occurs at a higher rate for adiabatic expansion. Of course, once recombination starts, the plasma does not continuously move along its adiabat, and so this discussion can only indicate the characteristic behaviour in a very simplified way.

We now compare stellar envelopes with the same *radius* and for the same heating rate. Note that these stars may have received a different total heating energy input from each other when they have the same radius, but this difference is small before the envelope expansion settles to a self-regulated solution or starts to run away.

For bottom-heating cases, due to the ongoing convection (see Section 6.1), the envelopes are almost ideally isentropic both in space (throughout the envelope) and in time (see Fig. 6). On the other hand, the cases with uniformly distributed heating form strongly non-isentropic envelopes, also both in space and in time. Hence, when stars with the same radius and which are heated at the same rate are compared, $F(\rho, T)$ values in the bottom-heated cases are overall smaller than in stars with significantly non-isentropic envelopes. In addition, the $F(\rho, T)$ derivative with respect to mass is smaller in isentropic envelopes – it is more nearly constant over a larger mass range within the envelope. Because hydrogen recombination follows $F(\rho, T)$, at any instant in an isentropic envelope: (i) hydrogen is recombining in a larger range of mass and (ii) the envelope is overall more recombined than in a non-isentropic envelope with the same radius.

Whilst this analysis is very simplified, this difference in behaviour is present in our simulations that use complete EOS. We see a noticeable difference in $F(\rho, T)$ values and profiles when comparing these two types of envelopes. The difference can be obvious when the stars have only expanded to 200 $\mathrm{R}_\odot$, well before the expansion starts to run away.

For envelopes with the same radius, we therefore expect that the rate of recombination energy release is greater in isentropic envelopes. Accordingly, we see higher local values of $\varepsilon_{\mathrm{rec,\,H}}$ at every single moment in the calculations of isotropic envelopes (i.e. those with bottom heating) than in the non-isentropic envelopes (i.e. those with uniform heating).

We estimate the local rate of energy input which is capable of disturbing local hydrostatic equilibrium as $\varepsilon_{\mathrm{pot}} = GM/(r\tau_{\mathrm{dyn}}(r))$ (comparable to the global dynamical luminosity L_{dyn}, as defined earlier). This provides a natural scale to which we can compare the local rate of energy release from recombination, $\varepsilon_{\mathrm{rec}}$. Comparing two stars heated at the same total rate and with the same stellar radius, we find that models with adiabatic envelopes have a significantly higher $\varepsilon_{\mathrm{rec}}/\varepsilon_{\mathrm{pot}}$ than those with non-adiabatic ('entropy-bubble') envelopes. For those adiabatic envelopes, the ratio $\varepsilon_{\mathrm{rec}}/\varepsilon_{\mathrm{pot}}$ can be as high as 10. When $\varepsilon_{\mathrm{rec}}/\varepsilon_{\mathrm{pot}} \gg 1$ in a substantial part of the envelope, then hydrogen recombination provides 'dynamical' heating, and the envelope expansion runs away. (Recall that isentropic envelopes tend to show significant recombination over a relatively large range of masses, which also helps to produce this outcome.)

From all of the above, we conclude the radiative zone which develops in uniformly heated envelopes is key in slowing down the overall rate of recombination and consequently prevents runaway expansion.

6.4 Supersonic and super-Eddington convection and mass-loss

While in the uniform case the luminosity increases towards the surface, in the bottom heating the luminosity decreases towards the surface. Within radiative zones, as expected, the luminosity is always locally sub-Eddington (here the local Eddington luminosity was calculated using local opacities). However, for bottom heating, the local luminosity in convective zones can be substantially super-Eddington.

When the internal heating becomes sufficiently high, the outwards energy flux may also exceed the amount which normal subsonic convection described by the mixing length theory would be capable of carrying (see Fig. 8). A similar problem is known to occur sometimes in very massive stars when neither subsonic convection nor radiation can carry all of the required energy flux (Quataert & Shiode 2012; Shiode & Quataert 2014). If that joint condition on radiative and convective energy transport is met when the star also has a surface radiative zone, it has been argued that wave-driven mass-loss will occur (Quataert & Shiode 2012; Shiode & Quataert 2014). The rate of this mass-loss has been predicted to be as large as 1 $\mathrm{M}_\odot\,\mathrm{yr}^{-1}$ (Quataert & Shiode 2012; Shiode & Quataert 2014). While this situation does not occur in all the models we considered, it did happen for Cases 2, 3 and 4 (uniform heating), and for three variations of the Case 2 bottom-heating model (X6, X8 and MS015). The luminosity at the top of the convective zone is usually up to a few times larger than the local Eddington luminosity,

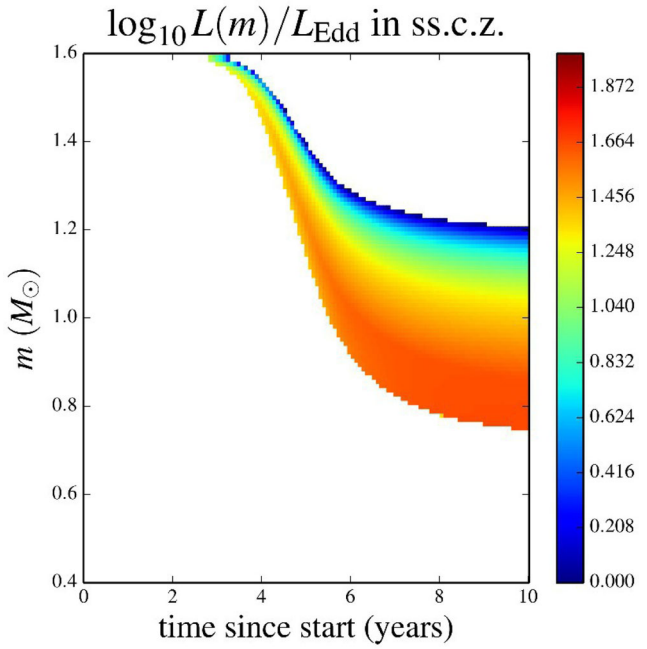

Figure 8. The ratio of the local luminosity to local Eddington luminosity, shown only for those convective regions where subsonic convection cannot carry the energy flux anymore for the uniform heating Case 4.

suggesting that the heated envelope may experience substantial wind mass-loss.

6.5 Growth of instability

Hydrogen recombination plays the most important role in the overall formal instability of the envelope – in the region of partial hydrogen recombination, Γ_1 is minimal (see Fig. 9). The integral of this quantity inwards from the surface, $\langle\Gamma(m)\rangle$, implies that most of the envelope in almost all of the models we calculated is formally dynamically unstable (the only exception is that of Case 5 with uniform heating – 'dynamical' heating). We stress that we are not referring here to the importance of hydrogen recombination to the *energetics* of ejection, but to the value of Γ_1.

6.6 Pulsations

While we anticipate dynamical instability of the envelopes in general, we have also encountered *relaxation pulsations* in our calculations. The pulsations take place at the moment when the stellar radius is about to reach self-regulation (in terms of radiating away the heating luminosity). If the star expands too fast at this point, the expansion runs away. If the star is expanding sufficiently slowly, the transition from expansion to a self-regulated state takes place without noticeable pulsations. For intermediate rates of expansion, the stellar envelope first overshoots the self-regulated radius and then contracts back below the self-regulated radius. Obvious pulsations were first noticed in cases X6, X8 and MS015. The contraction phase of each pulsation is accompanied by *reionization* of the material all the way towards the bottom of the envelope, and therefore also involves helium reionization (see Fig. 10), which absorbs energy.

6.7 The core and its energy

It has previously been unclear whether the response of the core during CEEs might significantly affect the energy budget of envelope ejection (see e.g. Ivanova et al. 2013a). In all of our simulations, the total binding energy of the core became only slightly *less negative*. We presume that this energy was taken from nuclear energy release, although we cannot be sure. However, the accumulated difference in binding energy is roughly 0.05×10^{46} and hence is small compared to the other terms in the energy budget which are discussed elsewhere in this paper.

6.8 Are these results unique to this particular choice of the core mass?

We have recalculated several examples using different initial stellar models, specifically ones with a smaller core mass (since it has broadly been expected that recombination energy will be more significant for CEE involving giants with larger radii). We applied similar prescriptions in terms of the heating rate per unit of time and the mass distribution (i.e. with the heating confined to the bottom $0.1\,M_\odot$ or spread through the entire envelope). We obtained strikingly similar results. The outcomes were qualitatively the same, in that the same heating rates resulted in either runaway or self-regulated outcomes as in our standard models, albeit at different values of $E_{\rm heat}^{\rm gross}$. In some respects they were also quantitatively very similar, since the steady-state luminosities and radii were roughly the same as in our base case (they were slightly lower by an amount which corresponds to the lower nuclear luminosity of the initial model). For such smaller core masses, the initial binding energy of the envelope is significantly more negative. The final outcomes for these models take place at slightly higher values of $E_{\rm heat}^{\rm gross}/E_{\rm bind}$ than in the comparable standard models.

7 CONCLUSIONS

We have studied simplified models of the phase of CEEs which is expected to follow the initial dynamical plunge. These calculations suggest that such heating could produce two types of outcome:

(i) 'runaway' – the envelope expansion accelerates until it starts to escape on its current dynamical time;
(ii) 'self-regulated' – the envelope expands enough to radiate away the heating luminosity. However, even in these cases most of the envelope becomes formally dynamically unstable.

Which of these outcomes occurs is determined not only by *how much* heating energy is provided to the star, but is strongly dependent on *where* and *at which rate* the heating energy is provided.

In all the cases we considered, the envelope either reached runaway expansion or a formally dynamically unstable state of self-regulation after receiving *less* net heating energy than the initial binding energy of the envelope (where we define this binding energy as gravitational potential energy plus internal thermal energy but without the recombination energy terms). This confirms that the release of recombination energy can be energetically important to CE ejection.

To quantify and illustrate the approximate importance of recombination, we define the efficiency $\eta_{\rm min}$ – the ratio of the *gross* heating luminosity to the binding energy (again including only gravitational and thermal terms in $E_{\rm bind}$, without recombination energy). Then the standard energy formalism can be rewritten as

$$\alpha_{\rm CE}\Delta E_{\rm orb} = \eta_{\rm min} E_{\rm bind}. \quad (20)$$

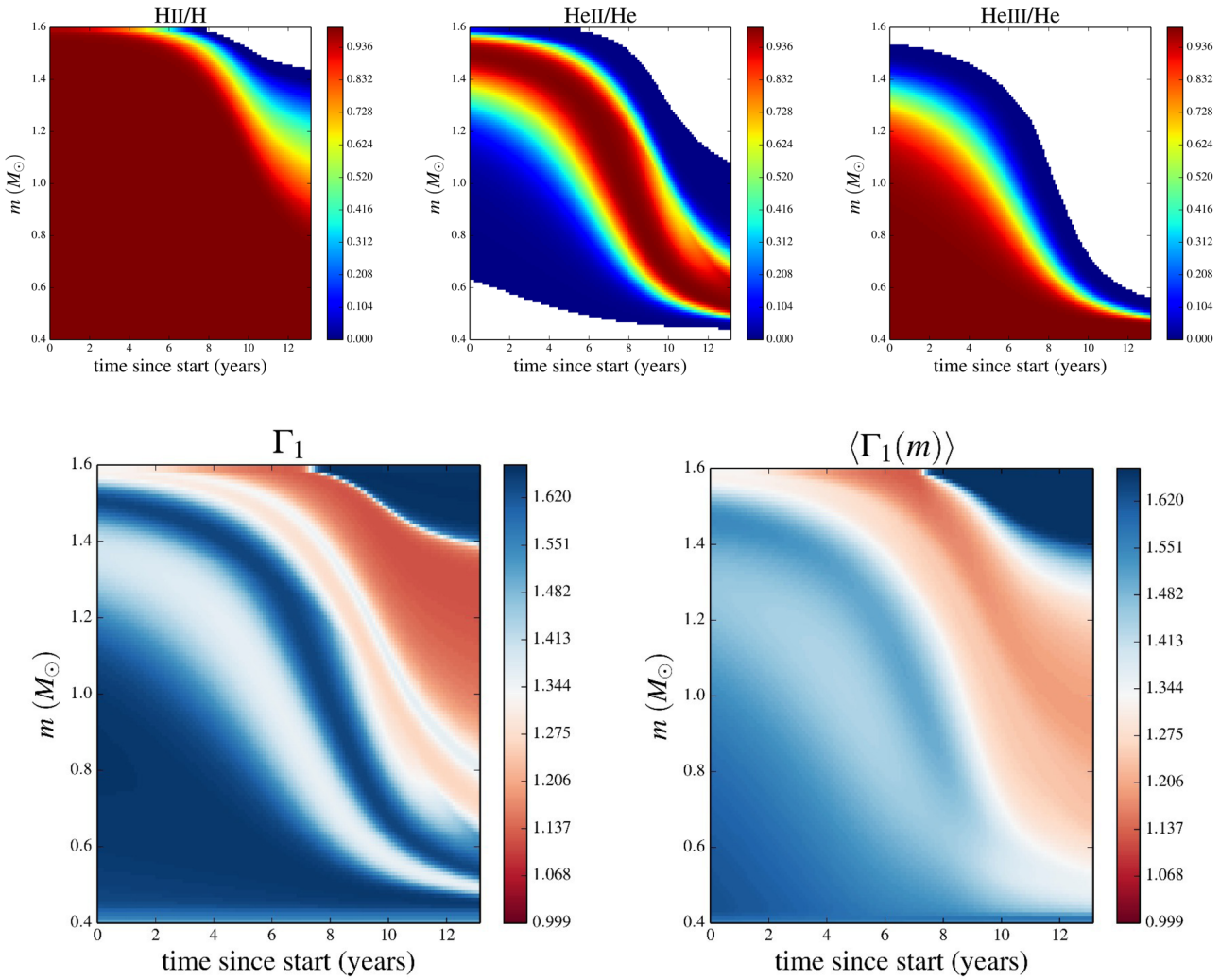

Figure 9. Ionization fraction of hydrogen and helium, local Γ_1 and integrated from the surface pressure-weighted volume-averaged $\langle\Gamma_1(m)\rangle$ in the Cases 3 uniform heating.

When some of the heating occurs close to the surface, the star can enter an energetically 'self-regulated' state in which the expanded star radiates away all the additional energy input. However, even during this 'self-regulated' stage, the envelope is formally dynamically unstable.[3] As much as 90 per cent of the envelope can be dynamically unstable for $\eta_{\rm min} \approx 75$ per cent. These envelopes may also experience strong mass-loss due to wave-triggered winds (see Section 6.4), or from Mira-type winds.

Importantly, we find that a higher heating rate makes the same amount of input energy more effective. Less massive secondaries are expected to plunge-in faster, and a smaller fraction of the gravitational energy release seems likely to be dissipated in the outer parts of the envelope. This suggests that the orbital energy release from relatively less massive secondaries might be more effectively used in removal of the envelope (see also Podsiadlowski 2001).

[3] Whilst this apparent self-regulation of radius expansion is not caused by the same mechanism as the self-regulation in Meyer & Meyer-Hofmeister (1979), we note that our results are directly relevant to that phase of slow spiral-in. In particular, we consider it very likely that the solutions of Meyer & Meyer-Hofmeister (1979) are close to formal dynamical instability.

We note that this argument qualitatively fits the inference from observations that the ejection efficiency grows when the companion is less massive (De Marco et al. 2011). However, we stress that De Marco et al. (2011) suggested that a low-mass companion would orbit for longer and that the longer time-scale would allow a giant to use its thermal energy, while our results suggest that a shorter time-scale for the spiral-in leads to a higher efficiency in the use of recombination energy.

Further studies of these relative ejection efficiencies will require the use of realistic frictional luminosity distributions. It might be that in some cases viscous heating occurs through a large fraction of a differentially rotating envelope, whilst in others the heating is dominated by dissipation close to the secondary. For example, the in-spiral of relatively more massive secondaries may tend to generate more broadly differentially rotating envelopes. If so, the envelope heating may be comparatively more widely distributed during the in-spiral of relatively more massive companions. Our calculations indicate that this would further reduce the envelope ejection efficiency of more massive companions, in addition to the differences caused by different in-spiral time-scales.

The ionization state of hydrogen plays two distinct roles in the outcomes of our calculations. Most clearly and generally, it is most

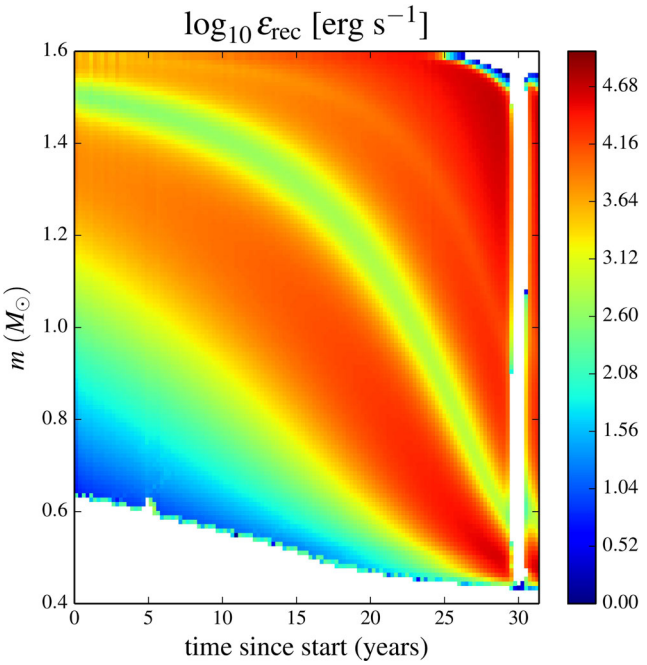

Figure 10. The rate of recombination energy release during the pulsations displayed by model X6. The blank vertical region at roughly 30 yr occurs during the contraction phase of the pulsation, during which matter is reionized and absorbs energy.

important in controlling for how much of the envelope the value of $\langle\Gamma(m)\rangle$ is low enough to indicate formal dynamical instability. In addition to that, our models sometimes show hydrogen recombination fronts which produce dynamically dominant rates of heating (see Section 6.3). Once hydrogen recombination is triggered in a dynamical mode, we speculate that this may be capable of removing the entire envelope, although our models cannot yet confirm this. Such dynamical hydrogen recombination fronts can be triggered in our calculations for $\eta_{\rm min} \approx 65$ per cent.

We stress that higher heating rates lead to lower $\eta_{\rm min}$. Heating which is confined to the lower half of the envelope – which seems likely for low-mass companions – may trigger dynamical hydrogen recombination at heating luminosities as low as 2×10^{45} erg yr^{-1}. For our initial stellar model, this heating rate could be provided by the spiral-in of a $0.3\,{\rm M}_{\odot}$ companion over a time-scale as long as 500 yr.

We expect that first-ascent giants with more massive cores (i.e. stars in which the potentially available recombination energy is a larger fraction of the initial binding energy of the envelope) would require even smaller $\eta_{\rm min}$ to produce each of the qualitative outcomes. However, we do not expect the change in $\eta_{\rm min}$ with stellar radius (or core mass) to be linear.

We have argued that differences in the progress of hydrogen recombination are primarily responsible for determining which of the qualitatively different outcomes occur. These differences are in turn a consequence of the entropy profiles and convective-radiative structures of the envelopes (see Sections 6.1 and 6.3). However, we have not been able to easily parametrize the importance of hydrogen recombination, either to the energetics or the stability of envelope ejection. The total energy released from recombination of hydrogen by the end of the simulations varied from 1 to 60 per cent of the initial energy reservoir. Nonetheless, we consider that the most important effect of hydrogen recombination effect is the way in which the ionization state controls the formal dynamical stability of the envelope. This dynamical destabilization takes place when hydrogen is still almost fully ionized. The understanding of the role of hydrogen recombination requires further study.

On the other hand, it is clear that in most cases, independent of both the location and amount of heating, and also independent of the qualitative outcome of the calculations (i.e. 'runaway' or 'self-regulated'), about 90 per cent of the recombination energy which was initially stored in ionized helium is used to expand the envelope. This apparently robust result suggests that it is safe to include helium recombination as an additional energy source in the energy budget for CE ejection when CEEs proceed past the dynamical plunge-in stage.

Our results therefore support the use of this recombination energy when CEE outcomes are estimated by use of an energy formalism. However, in order to start helium recombination, we expect that the companion should already have plunged deep inside the envelope, even for envelopes which could be described as initially 'unbound' if their recombination energy were taken into account (e.g. AGB stars). So our results should not be taken to support the notion that release of recombination energy can lead to envelope ejection without significant orbital shrinkage.

ACKNOWLEDGEMENTS

It is a pleasure to thank the anonymous referee for their positive and helpful suggestions. NI thanks NSERC Discovery and Canada Research Chairs Program. SJ thanks the Chinese Academy of Sciences and National Science Foundation of China, project numbers 11250110055 and 11350110324. PhP thanks the Umezawa Fund for hospitality. This work was supported in part by the National Science Foundation under Grant no. NSF PHY11-25915, Grant no. PHYS-1066293 and the hospitality of the Aspen Center for Physics.

REFERENCES

De Marco O., Passy J.-C., Moe M., Herwig F., Mac Low M.-M., Paxton B., 2011, MNRAS, 411, 2277
Deloye C. J., Taam R. E., 2010, ApJ, 719, L28
Fox M. W., Wood P. R., 1982, ApJ, 259, 198
Han Z., Podsiadlowski P., Eggleton P. P., 1994, MNRAS, 270, 121
Han Z., Podsiadlowski P., Eggleton P. P., 1995, MNRAS, 272, 800
Han Z., Podsiadlowski P., Maxted P. F. L., Marsh T. R., Ivanova N., 2002, MNRAS, 336, 449
Ivanova N., 2002, DPhil thesis, Univ. Oxford
Ivanova N., 2011, ApJ, 730, 76
Ivanova N., Chaichenets S., 2011, ApJ, 731, L36
Ivanova N., Taam R. E., 2004, ApJ, 601, 1058
Ivanova N. et al., 2013a, A&AR, 21, 59
Ivanova N., Justham S., Avendano Nandez J. L., Lombardi J. C., 2013b, Science, 339, 433
Kutter G. S., Sparks W. M., 1972, ApJ, 175, 407
Kutter G. S., Sparks W. M., 1974, ApJ, 192, 447
Ledoux P., 1945, ApJ, 102, 143
Lobel A., 2001, ApJ, 558, 780
Meyer F., Meyer-Hofmeister E., 1979, A&A, 78, 167
Paczyński B., 1969, Acta Astron., 19, 1
Paczynski B., 1976, in Eggleton P., Mitton S., Whelan J., eds, Proc. IAU Symp. 73, Structure and Evolution of Close Binary Systems. Reidel, Dordrecht, p. 75
Paczyński B., Ziółkowski J., 1968, Acta Astron., 18, 255
Passy J.-C. et al., 2012, ApJ, 744, 52
Pavlovskii K., Ivanova N., 2014, ApJ, preprint (arXiv:1410.5109)

Podsiadlowski P., 2001, in Podsiadlowski P., Rappaport S., King A. R., D'Antona F., Burderi L., eds, ASP Conf. Ser. Vol. 229, Evolution of Binary and Multiple Star Systems. Astron. Soc. Pac., San Francisco, p. 239
Quataert E., Shiode J., 2012, MNRAS, 423, L92
Ricker P. M., Taam R. E., 2008, ApJ, 672, L41
Ricker P. M., Taam R. E., 2012, ApJ, 746, 74
Shiode J. H., Quataert E., 2014, ApJ, 780, 96
Soker N., 2008, ApJ, 674, L49
Sparks W. M., Kutter G. S., 1972, ApJ, 175, 707
Stothers R. B., 1999, MNRAS, 305, 365
Tauris T. M., Dewi J. D. M., 2001, A&A, 369, 170
Tuchman Y., Sack N., Barkat Z., 1978, ApJ, 219, 183
Tuchman Y., Sack N., Barkat Z., 1979, ApJ, 234, 217
Wagenhuber J., Weiss A., 1994, A&A, 290, 807
Webbink R. F., 2008, in Milone E. F., Leahy D. A., Hobill D. W., eds, Astrophys. Space Sci. Libr. Vol. 352, Short-Period Binary Stars: Observations, Analyses, and Results. Springer, Berlin, p. 233
Wood P. R., 1974, ApJ, 190, 609

SUPPORTING INFORMATION

Additional Supporting Information may be found in the online version of this article:

Som (http://mnras.oxfordjournals.org/lookup/suppl/doi:10.1093/mnras/stu2582/-/DC1).

Please note: Oxford University Press are not responsible for the content or functionality of any supporting materials supplied by the authors. Any queries (other than missing material) should be directed to the corresponding author for the paper.

This paper has been typeset from a TEX/LATEX file prepared by the author.